Forging Topological Insulators on the Copper Surface State

Anthonie J J Harsveld van der Veen, B.Sc.

Condensed Matter and Interfaces
Debye Institute for Nanomaterials Science
Utrecht University, Netherlands

February 15, 2019

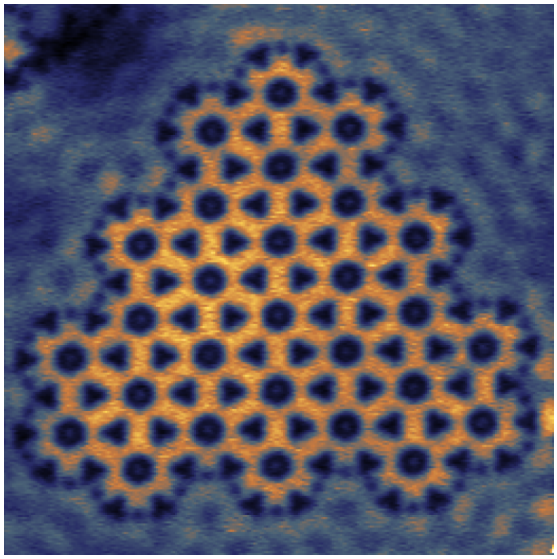

Master's Thesis
Supervisors:
S.E. Freeney M.Sc.
Prof. Dr. I. Swart
Prof. Dr. D.A.M. Vanmaekelbergh

Abstract

Artificial electronic lattices are quickly coming to the forefront of nanotechnological research. One form of particular interest for its low- resistance conductive properties is the topological insulator. In this thesis we consider the creation of a topological insulator in the shape of the Kekulé lattice. Using scanning tunnelling microscopy (STM) we were able to manipulate singular carbon-monoxide (CO) atoms on a copper (111) surface to confine the existing copper surface state into artificial atoms shaped into the Kekulé lattice. The Kekulé lattice was built in multiple variations to test for the existence and qualities of topological edge states based on the ratio of the nearest-neighbour hopping parameter T_0/T_1 and the influence of lattice geometry on the topological edge states. The existence of the topological edge state was confirmed using differential conductance mapping and spectroscopy and tested for robustness by introducing defects into the lattice. The lack of a topological edge state for the lattices designed to have none was confirmed using differential conductance mapping and spectroscopy. These practical results align strongly with theory and simulations done using tight binding (TB) and muffin tin (MT) calculation methods. With these results we hope to provide a basis for the realisation of artificial topological insulators and other conductive artificial systems.

Contents

1 Introduction

Advancements in the field of scanning tunnelling microscopy (STM) have opened up many new avenues of research. Beginning with studies of the shape of surfaces and the surface state in the 1980's [1][2], STM had grown into a discipline capable of manipulating individual atoms by the 1990's [3]. Using these manipulation techniques has allowed for the creation of many nano-scale structures made out of electron scatterers on conductive surfaces that reverberate throughout the scientific world such as possible electronic gates [4], artificial lattices such as molecular graphene [5], and from there even electronic fractal structures [6]. These artificial lattices are the focus of this research, as the electronic properties of nano-scale structures have become a subject of great interest in recent years, for which artificial lattices are a promising method of study.

The artificial lattices display a number of properties that push them to the front of the field. Foremost there is the tunability of these lattices. The electronic properties of graphene have been well documented [7] and are known to depend on the lattice parameters such as size of the unit cell. These same parameters can be varied to a high degree in artificial lattices, allowing for research into the electronic properties of different shapes and sizes. Research was done by Gomes *et al.* [5] into the creation of such an artificial lattice using carbon monoxide (CO) as an electronic scatterer on a copper (111) surface. The Cu(111) surface hosts a surface state in the energy range accessible using STM. This surface states forms a 2D electron gas (2DEG) with STM. Using the scattering properties of CO molecules, the 2DEG was confined into a molecular honeycomb shape, where electronic sites were substituted for the carbon molecules to form a honeycomb lattice akin to graphene. From this is was shown that the molecular graphene shows the same electronic structure found in "regular" graphene, namely the presence of Dirac-fermions. Matching of density of states (DOS) with tight-binding calculations for graphene show this method of artificial lattice creation to be viable for artificial graphene, and alludes to the same for many different structures [5]. In this research, we will focus on the topology of artificial lattices. Topology is the study of the shape of a space under continuous deformation. The topology of a system is one of many factors in the conductivity of the lattice on a conductive surface, as the deformation of space can be extended to the deformation of the band structure. Recent research in the field shows that this extends to artificial lattices by creating robust metallic edge states while maintaining insulating bulk to form the topological insulator. Such a material has almost zero-resistance conductivity in its edge-states, which opens up new areas in spintronics [8], nanoelectronics [9], and quantum computing [10]. A relatively simple graphene deformation that shows the influence of different topologies is the Kekulé distortion. Here the basic honeycomb symmetry is broken to create two classes of nearest-neighbour hopping; T_0 and T_1, where based on the assignment of these parameters one hopping will be larger than the other [Fig. 1]. This difference in parameter size will create a distinction between a pure insulator, and a topological insulator [5].

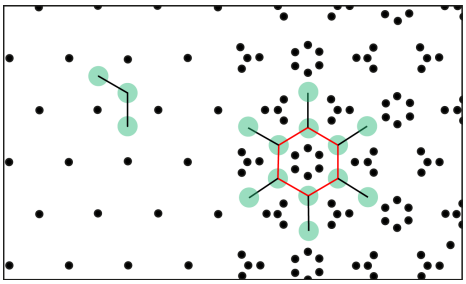

Figure 1: Schematic of lattice conversion from the triangular lattice (left) to the Kekulé distortion lattice. Artificial atoms are marked in green. Hopping parameters are shown between artificial atoms with equal hopping parameters in the triangular lattice and hoppings T_0 in red and T_1 in black in the Kekulé lattice.

The topological system is thus ripe for practical research. As defined by Gomes *et al.* and Kariyado and Hu, we will consider an artificial topological lattice one where the geometry of the lattice creates a variety in inter-molecular bonds. If this results in an artificial lattice that is insulating in the bulk and conductive at the edge, we consider the lattice to be a topological insulator[5][11]. While the first reviewed class of topological insulator was an alloyed material, for instance $Bi_{1-x}\ Si_x$ [12], the transition to purely artificial lattices for topological systems has great implications for the field as a whole.
The Kekulé lattice follows the described system of varying nearest-neighbour hopping parameters between artificial atoms. Gomes *et al.* demonstrated the principle by creating a "Mercedes"-arrangement within the basic graphene lattice made out of four CO-molecules [5], allowing for tuning of the nearest-neighbour hopping between hexagon-surrounding sites (intra-hexagon hopping) (red bonds in [Fig 1]), and nearest-neighbour hopping between two sites around different hexagons (inter-hexagon hopping) (black bonds in [Fig 1]). A detailed explanation of the topological phase in this system will be given in section 2.5. This method of creating a topological phase was followed in this research to remain consistent with the current standard, and to show the possible applications of the artificial CO lattice.

2 Theory

Here we will describe the theoretical basis of the research, starting with the basis of STM and adatom manipulation techniques, and take a close look at the process behind building lattices and specifically the Kekulé lattice.
The scanning tunnelling microscope has been in use since its creation in the 1980's [2][13][14] and has since been used for a wide variety of research. Recently interest in the creation of artificial lattices has grown rapidly, with the creation of the artificial graphene by Gomes *et al.* [5], the artificial Lieb lattice [15], and even the creation of electronic fractals using a CO lattice on a Cu(111) surface [6]. The Kekulé lattice is an interesting system with this progress in mind as a system that is producible in the STM and open to many different forms. Here we first focus on the armchair-edged Kekulé lattice before moving towards more advanced considerations with regard to topology such as not only the nearest-neighbour hopping parameters, but the shape of the edge as well.
The artificial atoms created in these lattices are so defined as a representation of actual atoms by a confinement of the Cu(111) surface state by CO scatterers. This modification and resulting properties of the surface state was shown by Gomes *et al.* to transform the massless Dirac fermions of the regular graphene lattice into massive Dirac fermions in the Kekulé lattice, which has been theoretically proposed to be a quantum phase transition [5][16] [17]. Combining the observed and prospected properties of the Kekulé lattice with research done by Kariyado *et al.* [18] into the origin of the topology and the influence of the edge shape of a lattice on the topology we are ready to bring the theory into reality.

2.1 Scanning Tunnelling Microscopy

Scanning tunnelling microscopy (STM) was first developed by Binnig and Rohrer [1] as a method to do high resolution surface studies. STM relies on the concept of electron tunnelling [1][2] as opposed to electron scattering or absorption in conventional electron microscopes. We assure a clean measuring surface in our STM by operating under ultra-high vacuum conditions, around 1×10^{-10} mbar or lower. The further underlying principle of STM is relatively straightforward; a conductive needle, or tip, is moved at a constant tunnel current or tip height over a conductive surface. The tip is connected to a piezoelectric drive, altering the height of the tip to maintain constant current, or the current to maintain constant height, resulting in a topographical image of the scanned surface. The relation between the current and distance of the tip to the surface is given as;

$$I \propto e^{-2\kappa d} \tag{1}$$

Where I is the tunnel current, κ is a decay constant, and d is the distance, showing the exponential relation between current and distance. The distance of this tip to the surface is typically in the order of Ångstroms, making a variation of one atom up or down greatly impact the tunnelling current. The topographical signal is visualised to show a reproduction of the scanned surface [1][2][13][14].

When the tip is terminated with a single atom, we consider it to be atomically sharp. An atomically sharp tip allows for atomic resolution, where one can see the individual atoms making up the surface.

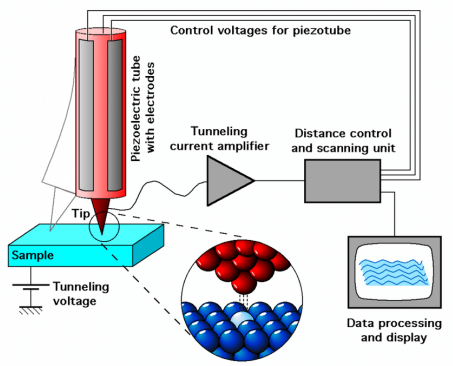

Figure 2: Schematic of an STM tip near a surface. Image by Md Nurul Huda [19]

2.2 Scanning Tunnelling Spectroscopy

A potent feature of the STM is the ability to perform *in situ* spectroscopy of samples using the basics of the scanning functionality with the addition of a lock-in amplifier. STM spectroscopy is a measure of differential conductance dI/dV[20], which is given as;

$$\frac{dI}{dV} = f_t(-V)f_s(0) + \int_{-V}^{0} dE f_t(E) f_s'(E+V)[20] \tag{2}$$

With f_t and f_s as functions of the tip and sample, respectively, and I defined as;

$$I(V) = \int_{0}^{V} dE f_t(E-V) f_s(E) = \int_{-V}^{0} dE f_t(E) f_s(E+V)[20] \tag{3}$$

In (1) and (2) we define *(V)* as the sample voltage relative to the tip, and E as the Fermi energy[20]. Where the first term in (1) is a counting term stemming from the change in tunnelling interval induced by a change in voltage [20]. The second term concerns the Fermi energies of the tip and sample, and the integrals disappear at vanishingly small voltages, leaving us with a single expression for the Fermi energies. If we sum over all such energies and assume spherical s waves for the tip, we find that this conductivity is proportional to the local density of states (LDOS) in the measured sample[20] [21]. An increase in the dI/dV thus indicates an increase in present electrons per area, which corresponds to a higher LDOS. The LDOS is a strong measure for conductance in the artificial lattices and thus valuable to measure. One downside to LDOS measurements

is that only the complete LDOS of a location can be measured, with no regard for the LDOS of the Cu(111) sample interference. This can be circumvented by taking spectra on a clean surface with the same tip and dividing the spectrum on an artificial atom by the obtained background. It is paramount to measure the background and desired spectra with the same tip, as the shape of the tip influences the measurements greatly as indicated via f_t in (1) and (2).
The DOS within the lattice of artificial atoms can also be visualised using differential conductance mapping, rather than differential conductance spectroscopy. Here a scan is made at a constant bias voltage, forming a topograph where areas of higher LDOS show clearly with higher intensity. This allows for identification of edge states by eye. We do not consider the presence of edge states in differential conductance mapping to be conclusive evidence of the presence of these edge states, or other states, but the visualisation is a clear indicator and should be indicative of their presence.

2.3 Adatom Manipulation

Atom manipulation using STM is done using what is termed a "tunable chemical bond"[22][23]. This bond is made between the end of the STM tip and the adatom, and can be tuned by the distance between the tip and adatom. The bond between the tip and adatom is established by the induced tunnel current through the tip. The adatom will be bound to both the tip and the substrate at first, allowing for so called *lateral manipulation* of adatoms [22][24][25]. The bond strength between the adatom and the tip might be increased to the point where the bond between the substrate and the adatom is broken, thus allowing the tip to carry the adatom separately as *vertical manipulation*[22][25]. While vertical manipulation is a less reliable method of manipulation, one can still build simple nanostructures using this method [22].
Three methods of *lateral manipulation* are possible; an adatom can be either pushed or pulled by the STM tip, or continuously drawn over the substrate surface as *dragging*[22][24][25]. Pulling an atom is done by inducing an attractive force between the STM tip and adatom through varying of the current, resistance, and tip-adatom distance. The tip is moved towards the desired direction in close proximity to the surface[24][25], inducing strong tip movement when moving over surface atoms and into appropriate adsorption sites. As the tip moves suddenly over a surface atom and into an adsorption site the adatom hops after it to fill the site [24][25]. Pushing of adatoms is done by using a repulsive force, induced in the same manner as the attractive force. Continuous manipulation is done using an attractive current once more. Here the tip is placed directly above the adatom and drags it over the substrate surface. For this project we use the *dragging* method of adatom manipulation for its reliability and further ease of use.

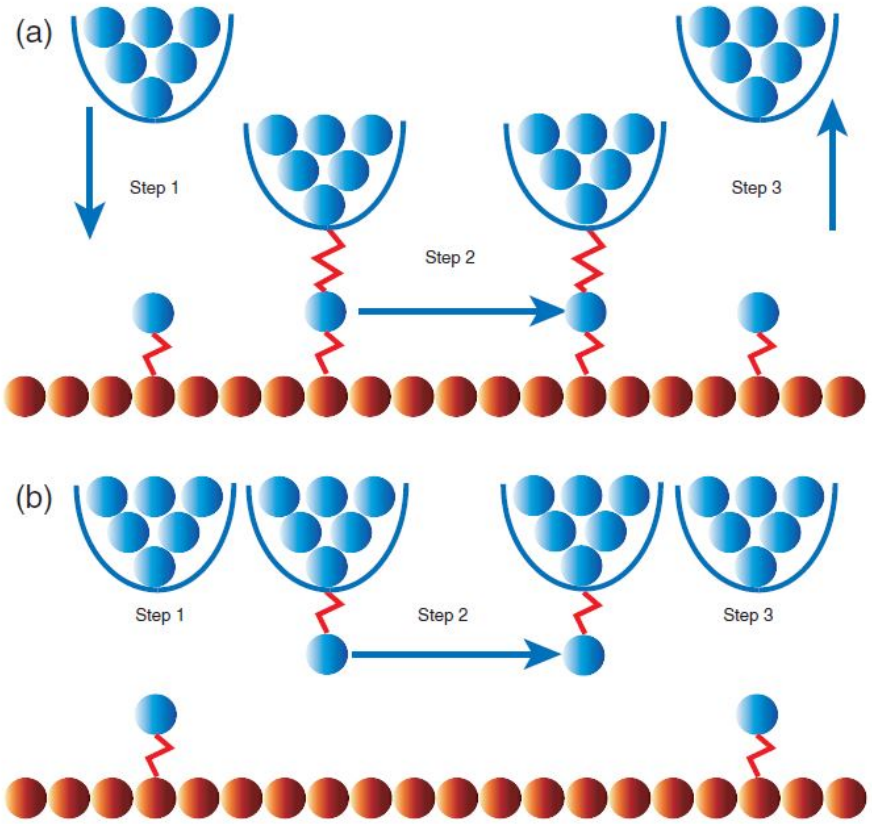

Figure 3: Schematic of (a) lateral (dragging) and (b) vertical adatom manipulation. In (a) step 1 is the approach of the STM tip into close enough proximity to bind the adatom. Step 2 is the induction of an attractive current and the dragging of an adatom along the surface. Step 3 is the retraction of the tip and final placement of the adatom. In (b) Step one is only positioning of the tip above the adatom without the approach seen in (a). Step two is the induced attractive tunnel current to lift the adatom from the surface, and placing the tip in the desired position. Step 3 is the release of the tunnel current, depositing the adatom at the new site. Image from *Invited Article: Autonomous assembly of atomically perfect nanostructures using a scanning tunnelling microscope* by R. Celotta *et al.*[22]

2.4 The Copper Surface State

The copper surface in use for these experiments was chosen for its present 2DEG. This 2DEG forms from the Cu(111) terminated surface exposed to the vacuum of the STM. As stated in **2.2**, this electron gas can be confined neatly by the use of scatterers to form artificial atoms of concentrated electrons on the copper surface. The copper surface has a clear DOS onset around -0.45V [Fig 4] and a heightened DOS over the entire voltage range, resulting in the need to normalise spectra taken on structures positioned on copper.

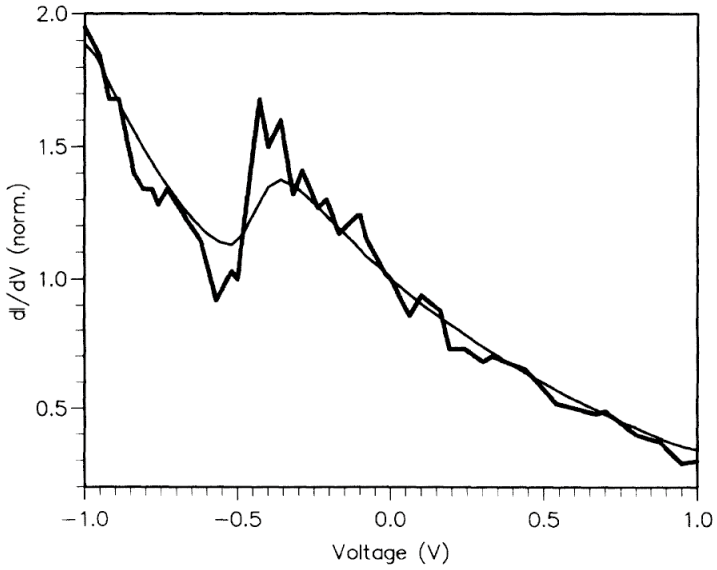

Figure 4: Differential conductance of a flat Cu(111) surface. The smooth line is a calculated conductance, the erratic line measurements showing great overlap. [20]

The structures we wish to create, as mentioned in **1**, are made as an arrangement of CO molecules. The CO arrangement is the inverse of the lattice we wish to create. The CO confines the surface state of the Cu(111) surface to a limited space, creating a cluster of electrons reminiscent of the electron cloud around a regular atom. In a triangular CO lattice on a Cu(111) surface, these atoms would form the honeycomb structure. This creates the molecular graphene lattice as shown by Gomes *et al.*[5]. For the Kekulé distortion, these clustered electrons take on the properties of a Dirac fermion at the edge of the structure, while not acquiring any radical new properties in the bulk of the lattice, and form a topological edge state [5][11].

2.5 The Kekulé Lattice

The Kekulé lattice, modelled after the original model of benzene as thought up by August Kekulé, gives us a system where we can easily tune the topology [5]. The basis of the topological phase is found in the alternating nearest-neighbour hopping parameters strength [Fig 5]. The hopping parameters are tuned with regard to the hopping found in regular graphene to be either stronger or weaker. Using a hexagonal CO configuration as centre to tune intra-hexagon hopping and a tetrapod configuration to tune inter-hexagon hopping, we create two opposite lattices that differ from graphene [5].

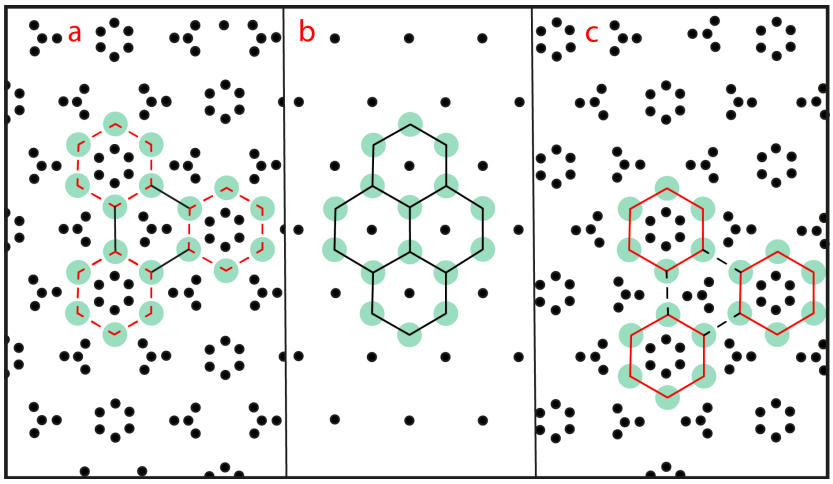

Figure 5: Schematic display of the hopping parameters in lattices with intra-hexagon hopping (red) smaller than inter-hexagon hopping (a), continuously equal hopping in the molecular graphene lattice (b), and intra-hexagon hopping (red) greater than inter-hexagon hopping (black) (c). Weaker hopping is indicated as dashed lines.

The correct ratios between these hopping parameters allows for the existence of a topological edge state. In literature [26] we find that a system is a topological insulator when the intra-hexagon hopping, henceforth T_0, is smaller than the inter-hexagon hopping, henceforth T_1;

$$T_0/T_1 \begin{cases} < 1 \rightarrow topological \\ > 1 \rightarrow trivial \end{cases}$$

Where a trivial system is a total insulator. As shown by Gomes *et al.*, a topological insulator can be built using the Kekulé lattice as a basis by exchanging singular CO molecules in a hexagon around a central CO with tetrapods [Fig 5a], tuning the nearest-neighbour hopping down between hexagonal sites. The hopping parameter relation created by Gomes *et al.* creates the mentioned dispersion in hopping strength in such a way that an energy gap is created and the

normally conductive properties of the molecular graphene lattice are suppressed [5].
Using the structure shown by Gomes *et al.* we devised to build both the topological and trivial Kekulé lattices on the Cu(111) surface. The artificial atoms created are defined by the Hamiltonian;

$$H = \epsilon \sum_i c_i^\dagger c_i + T_0 \sum_{\langle i,j \rangle} c_i^\dagger c_j + T_1 \sum_{\langle i',j' \rangle} c_{i'}^\dagger c_{j'} \tag{4}$$

where $c_i^\dagger$ is an operator that creates an electron at site i, with on site energy ϵ, $\langle i,j \rangle$ and $\langle i',j' \rangle$ run over all nearest neighbour sites, with intra-hexagon hopping energy T_0 and inter-hexagon hopping energy T_1 respectively. Here, the unit cell is defined as in [Fig 6] [26]. In the hexagonal unit cell, the middle four eigenstates form emergent orbitals that have pseudo spin and have pseudo-TR symmetry, resulting in a topological phase for $T_1 > T_0$. Note that the effective spin-orbit coupling, for small differences $\|t_0 - t_1\| = 0.1t_0$ in this system is ∼3000 times larger than the spin-orbit coupling in real graphene [26], resulting in a large topological gap, which is well suited for hosting the non-trivial topological system.

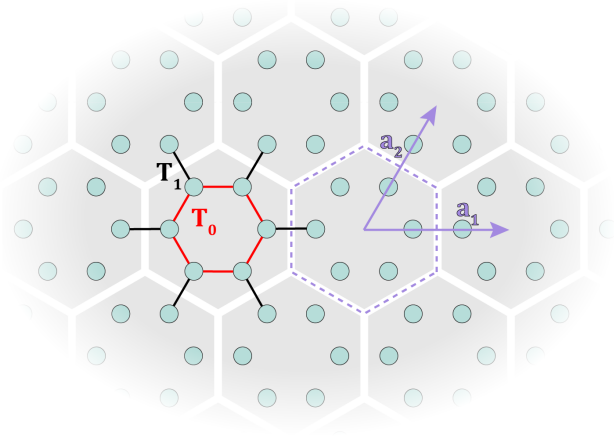

Figure 6: Detuned hopping in the honeycomb lattice. The lattice has primitive cells denoted by the grey hexagons and lattice vectors $\vec{a}_1$, $\vec{a}_2$. NN-hopping energies in the unit cell T_0, denoted with red bonds are detuned from the those out of the unit cell T_1 which are coloured black.

Combining the works by Gomes *et al.* and Wu *et al.*, we designed a trivial and non-trivial lattice suited for building on the Cu(111) surface [Fig 7].

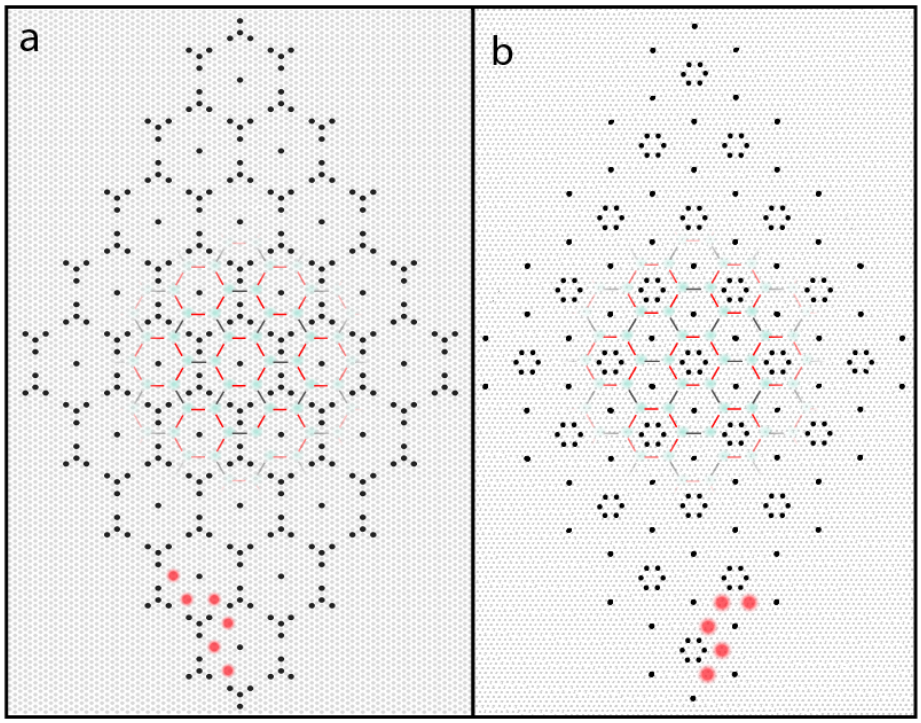

Figure 7: Schematic design for the trivial (a) and non-trivial (b) Kekulé lattices on a Cu(111) surface. The CO-scatterers are marked in black and show the anti-lattice. In both images the artificial atoms are marked in green, with the intra-hexagon hopping T_0 marked in red, and the inter-hexagon hopping T_1 marked in black. Large red dots at the edges in (a) and (b) give an easy view of the armchair-edge of these lattices. In (a) the intra-hexagon sites are strongly coupled, while the inter-hexagon coupling is weak as a result of tetrapod configuration showing a trivial lattice. In (b) the inter-hexagon hopping is markedly stronger than the intra-hexagon hopping, showing a topological insulator-lattice.

In (a) we show the topologically trivial lattice. Here the tetrapods as devised by Gomes *et al.* are arranged in a closed configuration, limiting nearest-neighbour hopping via T_1, creating the topologically trivial system, as T_0 around the single CO scatterer remains strong. We inverse these hopping strengths in (b) by replacing the central CO scatterer with a hexagon of CO's, effectively weakening T_0, and replacing the tetrapods with single CO molecules, strengthening T_1 to the desired ratio $T_0/T_1 < 1$, thus creating a theoretically topological insulator. Using these designs is highly advantageous for their high tunability, as the conversion from one lattice to another can be done swiftly without the need for higher CO coverage on the copper surface. With this we hope to show the basic viability of the topological lattice.

While the design so far shows great promise to have an insulating bulk and conductive edge states, the conductance via an edge instead of a large bulk area raises the question of the effect of edge shape on these states. The same question was raised by Kariyado and Hu [18] with regard to the shape of the edge of an infinite ribbon with tunable hoppings, and the origin of topologically insulating behaviour. Kariyado and Hu introduce us to new variables concerning the existence of the topological edge state, namely δ and the mirror winding number[18]. We define δ as;

$$\delta = \frac{T_1 - T_0}{T_0} \tag{5}$$

Where a system with $\delta = 0$ has no topological edge state. We define the mirror winding number as[18][27];

$$n(k_\parallel) = -\frac{1}{2\pi}\int_0^{2\pi} \frac{d}{dk_\perp} arg(detQ_{k_\perp,k_\parallel})dk_\perp \tag{6}$$

With $k_\parallel$ the momentum parallel to the unit vector a_1, $k_\perp$ the momentum perpendicular to the unit vector $\vec{a}_1$ [Fig 8, and Q_k the off diagonal factors of the Hamiltonian established by Kariyado and Hu for the vector $k_\parallel = 0$ [18]:

$$H_k = \begin{vmatrix} 0 & Q_k \\ Q_k^\dagger & 0 \end{vmatrix} \tag{7}$$

The factor Q is dependant on the hopping parameter ratio T_0/T_1 and the choice of unit cell made [18]. Here the Hamiltonian anticommutes with the chiral operator $\gamma = (1, -1)$, establishing a sublattice symmetry necessary for the calculation of the winding number. Considering only momenta perpendicular to $\vec{a}_1$, and mirror symmetry about $k_\parallel$, we can decompose Q into even and odd sections $Q^\pm_{k_\perp}$, which we can plug into **(6)** to find the separate mirror winding numbers (n_+, n_-).

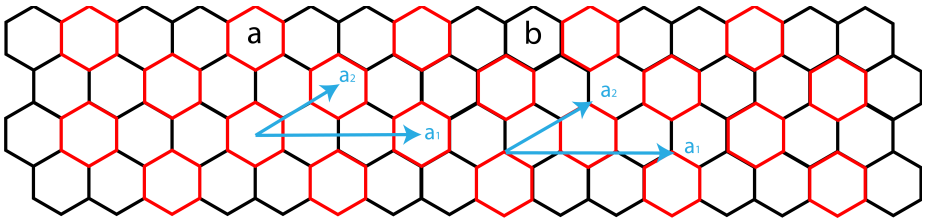

Figure 8: unit cells for the molecule-zigzag (a) and partially-bearded (b) edged lattices on an infinite ribbon with hopping parameters T_0 in **red** and T_1 in **black**

To demonstrate the effect of the edge geometry on a topological insulator, Kariyado and Hu created two types of edge, dubbed the molecule-zigzag and partially-bearded edges [Fig 9][18].

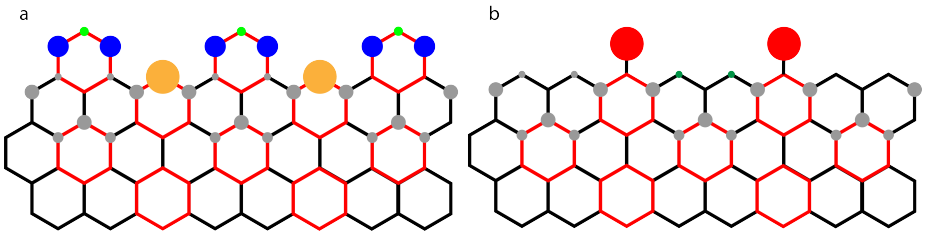

Figure 9: Schematic display of the molecule-zigzag (a) and partially-bearded (b) edges on infinite ribbons. In both artificial sites are marked, with size correlation according to expected DOS [18]. The bulk sites are marked in grey, the edge sites are marked in colour with same-type sites assigned the same colour.

It is shown that for both these edges an edge state appears when the correct ratio of hopping parameters T_0 and T_1 is applied via lattice adaptation. Considering the hopping ratio T_0/T_1 we find that for $\delta < 0$, the bearded edge is topological with $n_\pm = (-1, 1)$, thus giving a total mirror winding number 0 with non-zero individual winding numbers[18]. Here we also find $n_\pm = (0, 0)$ for the molecule-zigzag edge, implying that it has no topological edge state. If we find $\delta > 0$, the winding numbers for the molecule-zigzag edge will be $n_\pm = (1, -1)$, and we find the winding numbers $n_\pm = (0, 0)$ for the partially-bearded edge. This corresponds to a topological edge state for the molecule-zigzag edge when $T_0/T_1 < 1$, and a topological edge state for the partially-bearded edge when $T_0/T_1 > 1$. Kariyado and Hu postulate that it is not just the ratio of hopping parameter that determines the existence of topological edge states, but the shape of the unit cell, and per extension the edge, as well. With this in mind we set out to create a lattices with the proposed edge shapes. For the sake of symmetry we chose to create a triangle-shaped lattice in these instances, as a diamond-shaped lattice following the molecule-zigzag or partially-bearded edges could not be achieved [Fig 10] as in the armchair-edged Kekulé [Fig 7]. We propose the lattices shown in [Fig 10] will show an edge state for (a), and lack thereof for (b), as the proposed designs for the trivial and topologically non-trivial lattices in [Fig 7].

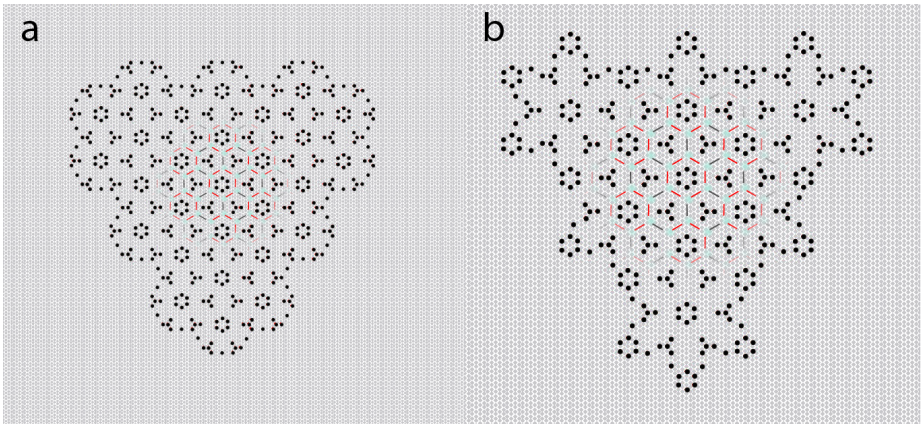

Figure 10: Schematic design of the molecule-zigzag (a) and partially-bearded (b) edges on a Cu(111) surface.Shown are the T_0 (red) and T_1 (black) nearest-neighbour hopping parameters from atomic site to atomic site (green).

In both designs the nn-hopping is tuned in the same way to give the same ratio of $T_0/T_1 < 1$, that would in theory produce a topological edge state in the armchair-edged lattice, indicating the effect the shape of the edge has on the topology of the system. Note that to ensure the edge states do not mingle with the surface state of the 2DEG blockers are introduced along the edge, confining the LDOS stronger than in the armchair-edged Kekulé. Kariyado and Hu note that there is no mirror operation for $k_{\|} = 0$ for the armchair edge, and no mirror symmetry [18]. The mirror winding number can not be calculated from **(5)**. This brings to doubt the topological qualities of the proposed armchair-edged Kekulé lattice. Would this lattice show no topological edge state, we can confirm the mirror winding number as a determining factor in the creation of topological insulators.

3 Methods

In this project we used the Low-Temperature Scanning Tunnelling Microscope (LT-STM) built by Scienta Omicron. Operations in the chamber were performed at ultra-high vacuum conditions (UHV) with a pressure range between 1×10^{-9} and 3×10^{-12} mbar. We do not consider this variation in pressure to be of influence on the experiments. The LT-STM operations were performed at 4.5 K. Two (111)-surface terminated pure copper crystals were used to build lattices on. Lattice building was done using a Pt-Ir tip coated in copper as a result of tip-sharpening. Control of the STM was held via MATRIX-software developed by Scienta Omicron. The Cu(111) crystals were cleaned with argon-sputtering/annealing cycles. For Ar-sputtering we used a voltage of 3kV with an emission current of 10 mA at 3.5×10^{-6} mbar pressure. For annealing a bias of 19.99 V with a current of 1.43 A was used. Sputtering/annealing cycles were set on 20 minute sputter, 5 minute anneal rotation and repeated until a clean surface was obtained. CO scatterers were added to the Cu(111) crystal by leaking of CO gas into the 4.5 K chamber to a pressure of 1.3×10^{-8} mbar for four minutes. STM topography was taken at a 0.1V bias with a current setting between 1 nA and 30 pA. Differential conductance maps were obtained by disengaging the feedback loop at a 1 nA current setpoint with a bias of 50 mV, after which the tip was approached in z-direction until a current of 200 pA was reached, then adjusting the bias to the desired value. Differential conductance mapping was done using an oscillating bias with integration time $T_c = 20$ ms. The sensitivity was set to 20 mV, and the oscillation amplitude A_o set at 10 mV scanned at a frequency of 273 Hz. Differential conductance spectroscopy was conducted using a raster time setting of 150 ms, scanning over a variation of bias ranges with a varying number of points at lock-in settings $T_c = 50$ ms, sensitivity 10 mV, $A_o = 10$ mV at a frequency of 273 Hz.

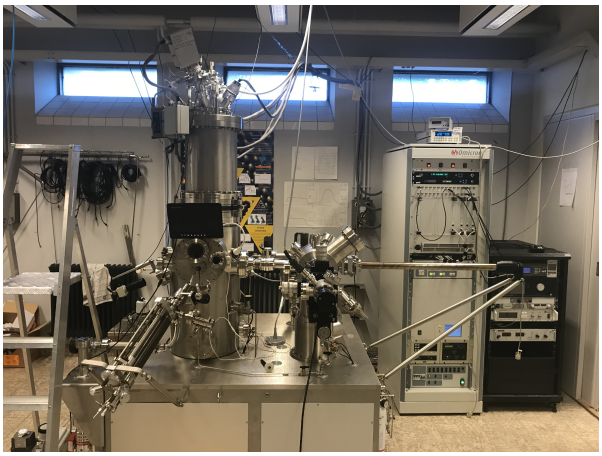

Figure 11: The LT-STM 'Dirac' system.

4 Results and Discussion

Using the STM, the various forms of the Kekulé lattice were built using CO as an electronic scatterer on a Cu(111) surface. Building was done following the design laid out in section **2.5** and following simulations using the muffin-tin method and the tight binding model discussed below.

4.1 Simulations

4.1.1 The Armchair Kekulé

Before physical building, Tight Binding (TB) and Muffin Tin (MT) calculations on various forms of the Kekulé lattice were done. First, calculations on the armchair-edged lattices for both the trivial and topological case were done to simulate both on a copper potential [Fig 12]. These calculations show an apparent edge state as was assumed from theory.

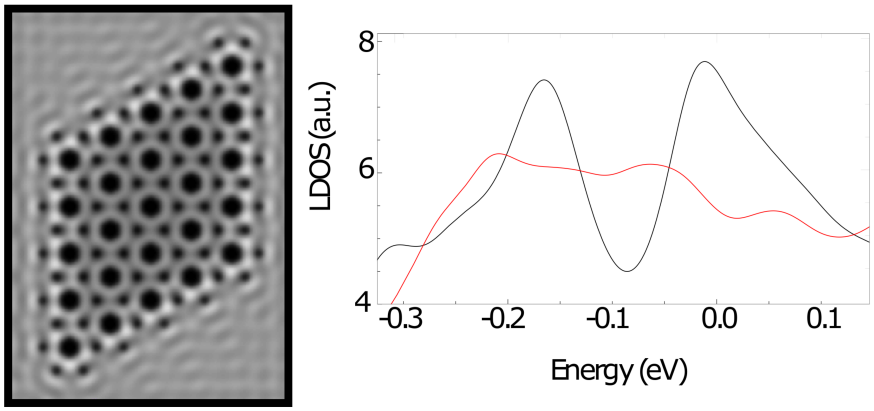

Figure 12: MT simulated image of the proposed topological Kekulé lattice (left), and a simulation of the LDOS (right). Here the spectrum in the bulk is shown as **black**, the spectrum on the edge is shown in **red**

In [Fig 12] we show the apparent edge state as a higher LDOS (red) within the projected gap for the bulk (black) of the Kekulé lattice at -0.065 eV. The same calculations for the trivial design as in [Fig 7(a)] show a DOS at the edge that matches the LDOS of the bulk, indicating that there are no edge states present. This is in line with the results produced by Gomes *et al.*[5] and the proposed influence of the tuning of the hopping parameter as a method to engineer topological edge states.

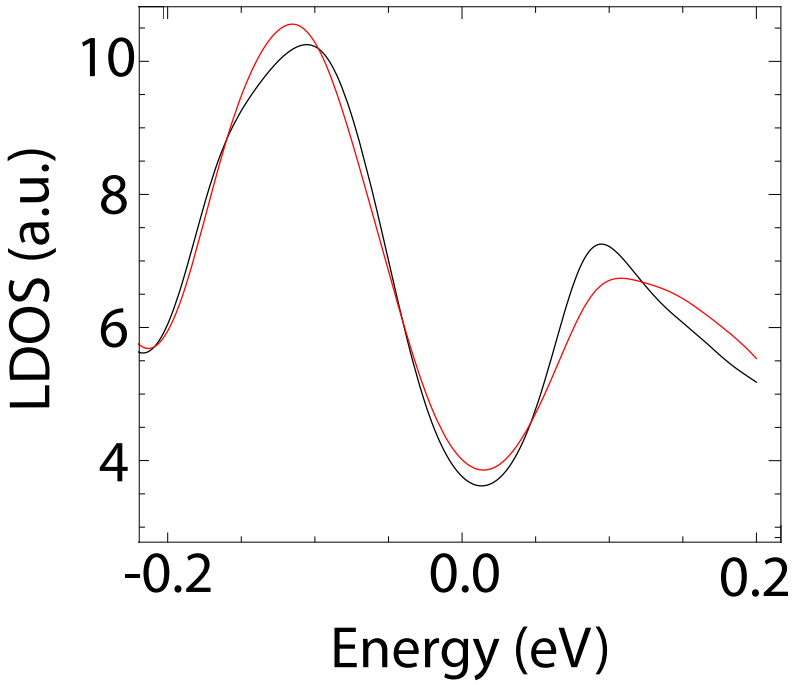

Figure 13: Simulation of the LDOS in the bulk (black) and at the edge (red) of the trivial Kekulé lattice.

A final simulation on these designs included defects in the topological armchair-edged Kekulé to show the edge state is robust, which is an integral quality of the topological edge state.Three defect types were introduced in an attempt to destroy the edge state; hopping blocking, site blocking, and boundary removal [Fig 14]. In the hopping blocking defect the space between sites has been occupied by a CO-scatterer to minimise the hopping parameter. A site blocking defect here shown is a CO-scatterer that occupies an artificial atom site wholly, removing it from the edge. Boundary removal defects remove the enclosure of the sites around the CO hexagons and open them up to the 2DEG for interference. In simulations none of these defects individually or combined caused a disappearance of the edge state. The simulated LDOS shows that the density of states remains heightened in the bulk gap when all types of defect are present, showing the robustness of the non-trivial lattice. From this we assumed the designs in [Fig 7] to be valid for the initial testing of the engineered topology. We resolved to use these designs on the copper surface using CO-molecules as scatterers.

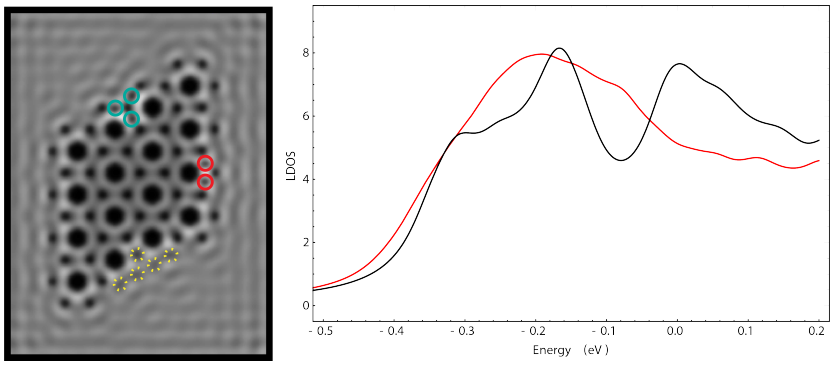

Figure 14: MT simulated dI/dV map of the non-trivial Kekulé lattice with defects (left) and a simulated LDOS plot (right). Here three types of defect are shown; hopping-blocking (cyan), site blocking (red), and boundary removal (yellow).

4.1.2 Edge-shape simulations

Using TB and MT methods simulations were done in collaboration with the Utrecht University department of theoretical physics [28]. These simulations were done on the different edge shapes as proposed by Kariyado and Hu [18]. From Kariyado and Hu we find not only a proposed shape for the topological insulators, but also and edge-related band structure. Band structures for the armchair, molecule-zigzag, and partially-bearded edges were calculated using tight-binding, showing expected edge-state presence for the hopping ratio $T_0/T_1 < 1$ [Fig 15].

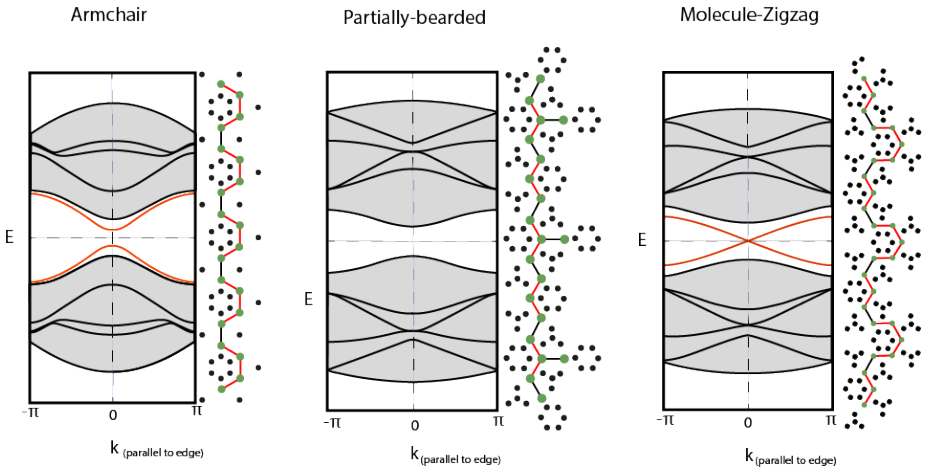

Figure 15: Simulated bandstructure plots for the armchair, partially-bearded and molecule-zigzag edge terminations of the topologically non-trivial Kekulé lattice. Connected to the bandstructure plots are the edges of the represented lattices, showing T_0 in red and T_1 in black, these bonds connecting artificial atomic sites marked green.

From [Fig 15] it shows that for the armchair configuration there appears to be a gapped bandstructure. This parallels the findings of *Kariyado and Hu*, where there were no mirror-winding number calculations possible on the armchair configuration for a lack of symmetry in the lattice [18]. We show that mirror-symmetry is absent in the armchair edge, showing it has no symmetry plane perpendicular to $\vec{a}_1$ as the molecule-zigzag and partially-bearded edges do [Fig 8]. We confirmed this by the bandstructures where it is shown that the partially-bearded edge has an open gap, indicating no conductance at the edge as proposed, while the molecule-zigzag edge shows a crossing band from the lower-to-higher energy and vice-versa, indicating a conductive state and thus the proposed edge-state. The open band in the armchair-edge points us towards the findings by Kariyado and Hu that not only the hopping parameter, but also the mirror winding number is crucial to the existence of the topological edge state. These findings throw into doubt the topological quality of the edge state

in the armchair-edged Kekulé. Practical results provide us with more detail on these findings in **4.2**.

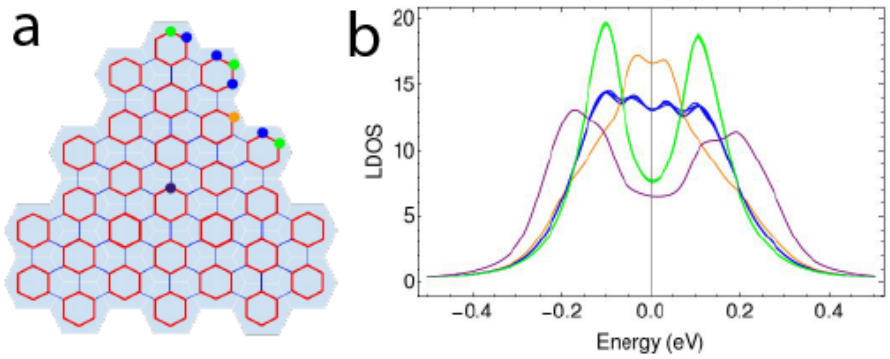

Figure 16: TB calculations of the molecule-zigzag-edged Kekulé lattice with $T_1 > T_0$. (a) shows a simple model of the Kekulé with T_0 in red and T_1 in blue. Four types of sites with distinct LDOS are indicated; corner (green), neighbour (blue), zigzag (orange), and bulk (purple). (b) shows the LDOS is arbitrary units on a -0.5 to 0.5 eV energy range. Colours in (b) correspond to sites indicated in (a)

Following the bandstructure-plots TB calculations on the molecule-zigzag were performed to show the expected LDOS [Fig 16]. In the bulk site we observe a lowered LDOS in [Fig 16b] around 0 V, while indicated neighbour (blue) and zigzag (yellow) sites show a heightened LDOS in this gap, indicating the presence of the edge state. Corner-type sites (green) do not show higher DOS around 0 V, instead showing us a definite energy gap. From this we noted the similarity to the energy solutions for trimer-molecules, and propose a formation of trimers on the edge of the lattice [Fig 17a]. Trimer molecules would show peak energy in equal states around 0 V as the corner-type sites show for -0.2 V and 0.2 V, but have a gap around 0 V, which is also shown. In the same fashion, the neighbour-type sites would show peak energies around 0 V and at 0 V, here displayed as well. In the trimer-model we consider the peak of the neighbour-type sites to split as an effect of coupling to the bulk, creating two peaks around 0 V instead of a single one on 0 V. Considering the edge sites of the molecule-zigzag lattice as a trimer site leads us to believe that we can consider the edge sites of the armchair-Kekulé as a dimer [Fig 17b].

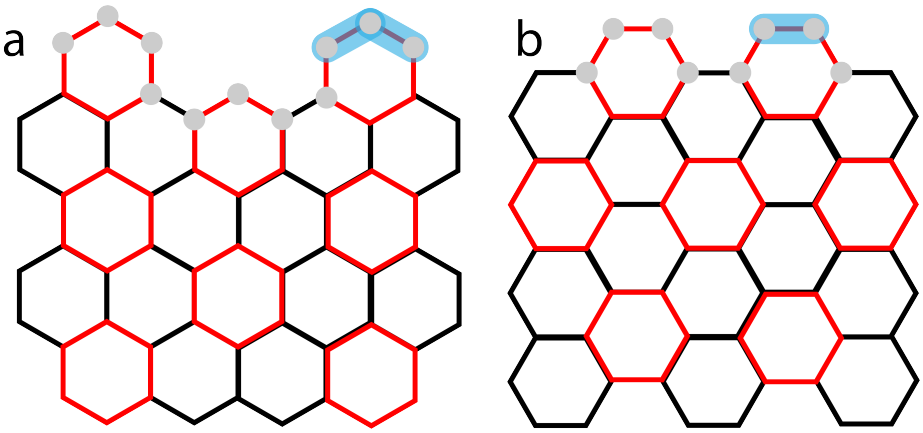

Figure 17: Proposed location of the trimer site on the molecule-zigzag edge (a) and dimer site on the armchair-edge (b) of the respective Kekulé lattices, indicated in blue.

The energy solution for a dimer is given as;

$$E_{\pm} = \alpha \pm \beta \tag{8}$$

with α the on-site energy and β the nearest-neighbour interaction energy terms of the dimer molecules, and E the energy eigenvalue. This shows the presence of a bonding and anti-bonding state in the dimer molecule as two separated energy levels. We expect no crossing takes place between these energy levels in the dimer. The bandstructure is thus gapped, presenting us with an edge state that is not topological in origin.
The energy solution for a trimer molecule is given as:

$$E_{\pm} = \alpha \pm \sqrt{2}\beta, E_0 = \alpha \tag{9}$$

With α the on-site energy and β the nearest-neighbour interaction energy, and E the energy eigenvalues. Here the next nearest neighbour hopping is set to 0. Solving for E shows three energy values indicates the existence of a bonding, anti-bonding, and 0 energy state. The 0 energy state allows for band crossing in the trimer and indicates the edge state here is topological in origin. We also note that the wavefunction of the E_0 energy level has a nodal point in the centre molecule, corresponding to the gap seen in the corner-type site DOS in [Fig 16b].

While a simulation for using the TB model shows a clear cut LDOS, the isolationist tendencies of this simulation are not wholly comparative to the reality of a lattice on a Cu(111) surface. The influence of the 2DEG on the lattice can not be ignored. A muffin-tin simulation of the lattice in a 2DEG yields a strongly broadened LDOS with regard to the TB calculations [Fig 18c], wholly obscuring the features observed in [Fig 16]. The interaction with the copper surface state can thus not be ignored, and to minimise this we resolved to put in additional CO scatterers to function as blockers for the surface-state-lattice interaction [Fig 18b,d]. Multiple iterations of the blocking can be found in supplement 2. Blocking close to the lattice was found to be most effective, shaping back the LDOS plot into one we recognise from TB calculations.A variety in intensity of different corner sites can also be observed in the TB simulated lattice [Fig 18b]. A shift with regard to the TB result still remains, which we prescribe to the remaining interaction with the 2DEG, which we can wholly tune out in TB simulations, but not in reality.

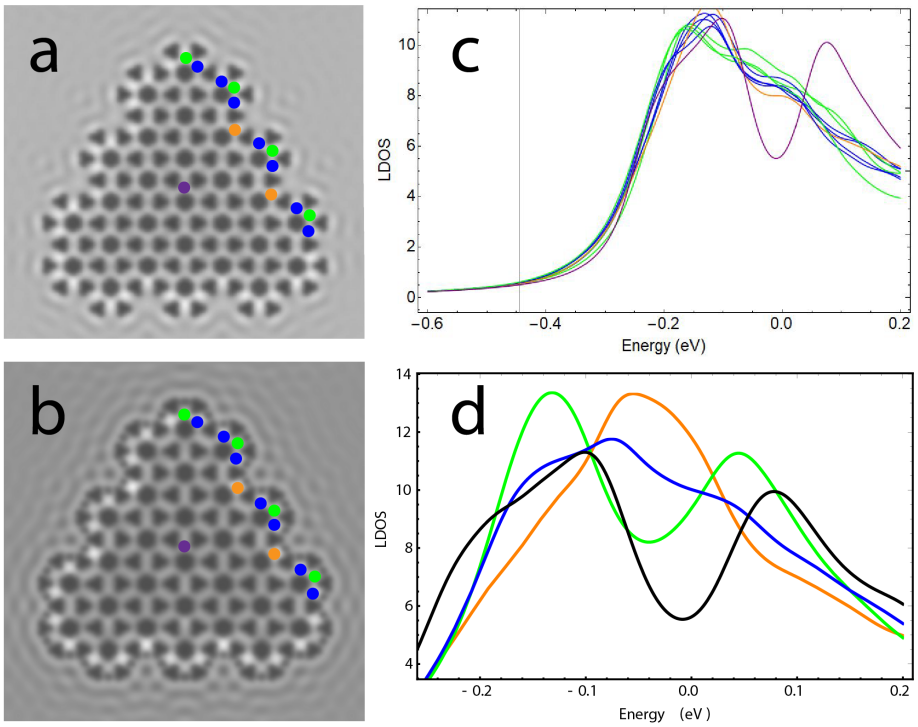

Figure 18: LDOS simulations using muffin-tin methods of the molecule-zigzag terminated Kekulé without blocking added (a) and with blocking added (b). Indicated in (a) and (b) are the corner (green), neighbour (blue), zigzag (orange), and bulk (purple) sites. Corresponding LDOS-spectra are shown in (c) and (d).

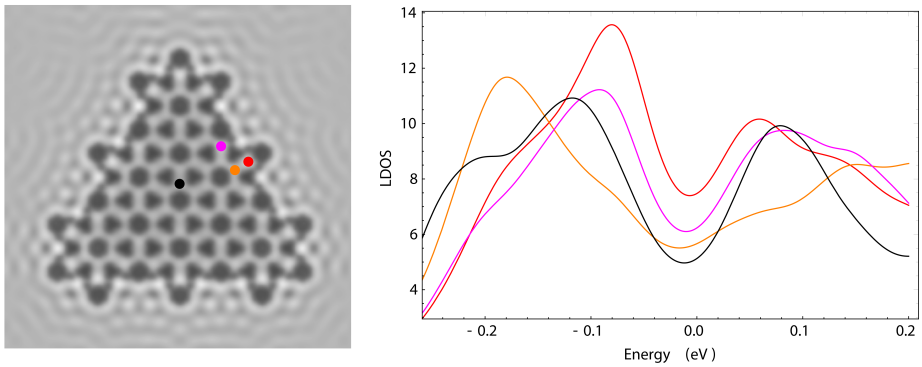

Figure 19: MT simulated image of the partially-bearded lattice and calculation of the LDOS of sites on the lattice edge.

MT calculations on the partially-bearded edge show an expected behaviour in LDOS [Fig 19]. All sites show varying LDOS across the energy range but display a clear gap around 0 eV, indicating that no topological edge-state exists. These simulated results are in line with the theoretical findings on the partially-bearded bearded edge, as well as expectations for the chosen hopping parameter ratio. The partially-bearded edge has also been blocked from the 2DEG using extra CO molecules in this model to remain consistent with theory and the molecule-zigzag-edge.
These simulations show that the creation of the topological forms of the Kekulé lattice as well as the topologically trivial lattice is possible using CO as a scatterer for the 2DEG on a Cu(111) surface. These simulations also show the effect of the lattice termination to the 2DEG in the form of the edge shape, and how the topological qualities are affected. Combining these findings with the findings in **4.1.1**, we are confident in building these lattices using the STM with observable results closely related to theory.

4.2 Practical Results

Below we discuss the practical results from the construction of the armchair, molecule-zigzag, and partially-bearded Kekulé lattices. While we attempted construction on the topologically trivial and non-trivial system for the armchair-terminated Kekulé, time constraints prevented us from the attempted construction of the molecule-zigzag and partially-bearded lattices with hopping parameters so that $T_0 > T_1$.

4.2.1 The Armchair Kekulé

Using the STM we were able to create the armchair-edged trivial and non-trivial Kekulé Lattices [Fig 20], using 220 individual CO molecules for the non-trivial system, and 305 individual CO molecules for the trivial system. No blockers were put in place in the building process for these lattices, which would allow for a coupling to the 2DEG in both. For the trivial design we consider this effect lesser, as the tetrapod configurations used to tune the hopping parameters act as an enclosure for the LDOS within the lattice. The LDOS of the edge in the non-trivial lattice is likely to have broadened as a result of this lack of blockers. The heightened intensity visible in [Fig 20b] on the outside of the trivial lattice may lead one to believe in the presence of an edge-state in this capacity, but we consider this to be a result of electron back-scattering of the 2DEG on the lattice border.

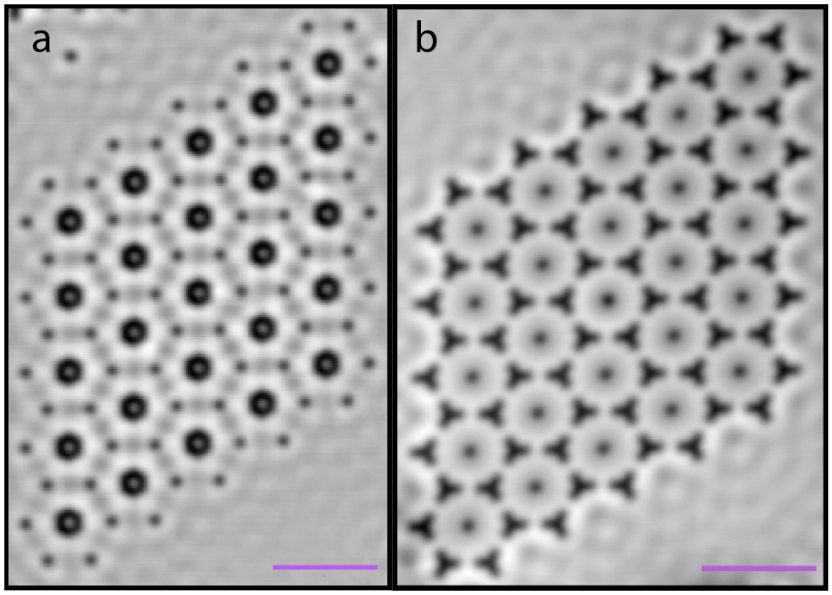

Figure 20: Topographs of the non-trivial (a) and trivial (b) Kekulé lattices taken at 100 mV on a Cu(111) surface. Scale bar displayed as 5 nm.

The non-trivial armchair-lattice has the proposed hopping ratio of $T_0/T_1 < 1$ as the inter-hexagon hopping as described in section **2** is only curbed via a single CO-blocker on either side of the bond. The intra-hexagon hopping is curbed by a central hexagon of CO molecules. Differential conductance mapping at -0.065V and -0.01V combined with STM spectroscopy over the range -0.6V to 0.5V show a clear presence of an edge state [Fig 21]. At -0.065V, the location in the experimental differential conductance spectrum where the gap between the bulk state and the edge state is largest, a clear heightened intensity is shown in [Fig 21a], while at -0.01V the LDOS of the bulk and edge have converged again to eliminate a specific edge state, shown as a uniform LDOS in [Fig 21b].

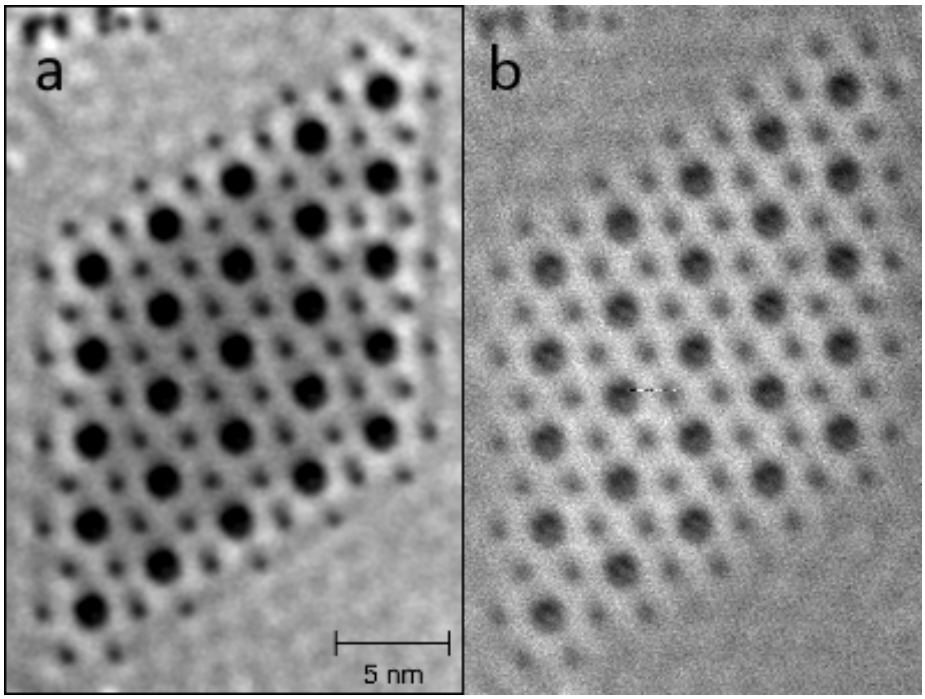

Figure 21: Differential conductance mapping at -0.065 V (a) and -0.01 V (b) of the topologically non-trivial Kekulé lattice.

The differential conductance spectroscopy taken on the lattice were averaged out over multiple spectra at the same location and normalised by dividing over spectra taken on the bare copper surface to show the LDOS of the lattice [Fig 22]. Here there is a clear difference in LDOS around -0.065V, strongly indicating of the edge state for this configuration of the Kekulé lattice. The measured dI/dV spectra also closely follow the simulated spectra shown in [Fig 12], where the bulk displays a strong peak before becoming gapped between -0.1 eV and 0 eV. The edge maintains a steady LDOS, crossing the DOS of the bulk around -0.1 V and crossing back again around 0 V, remaining in existence in the bulk gap.

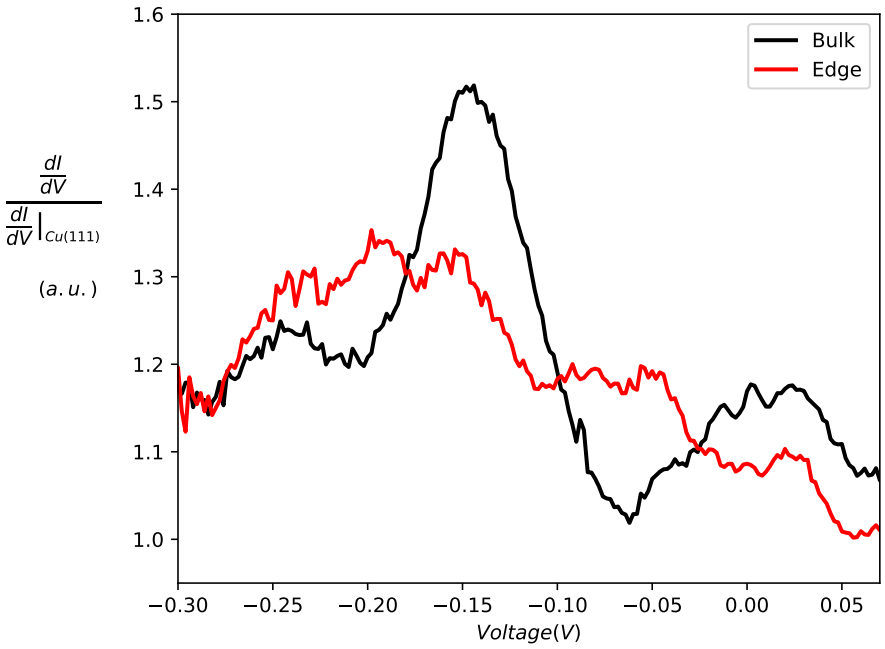

Figure 22: Averaged and normalised differential conductance spectra on the Kekulé lattice. The LDOS is displayed over a bias range of -0.3 to 0.1 V in arbitrary units. The spectrum in the bulk is marked **black**, the spectrum on the edge is marked **red**.

The trivial armchair-Kekulé lattice shows no edge state across a multitude of differential conductance maps [Fig 23]. As indicated by both theory and simulations, no edge state appears anywhere in the differential conductance mapping of the trivial lattice. Following the simulated LDOS progression in [Fig 13], varying intensity over the bias range is observed, but an edge state is never displayed. The dI/dV spectra of the trivial Kekulé confirm this observation [Fig 24]. The DOS at the edge follows the DOS in the bulk throughout the bias range, giving no indication of a present edge state. These differential conductance spectra are averaged out of multiple spectra and normalized against the copper background. The spectrum for the trivial Kekulé agrees with simulated LDOS plots from TB as well, showing the same shift in gap from -0.065 V to 0.0 V and same line up of the edge and bulk LDOS.

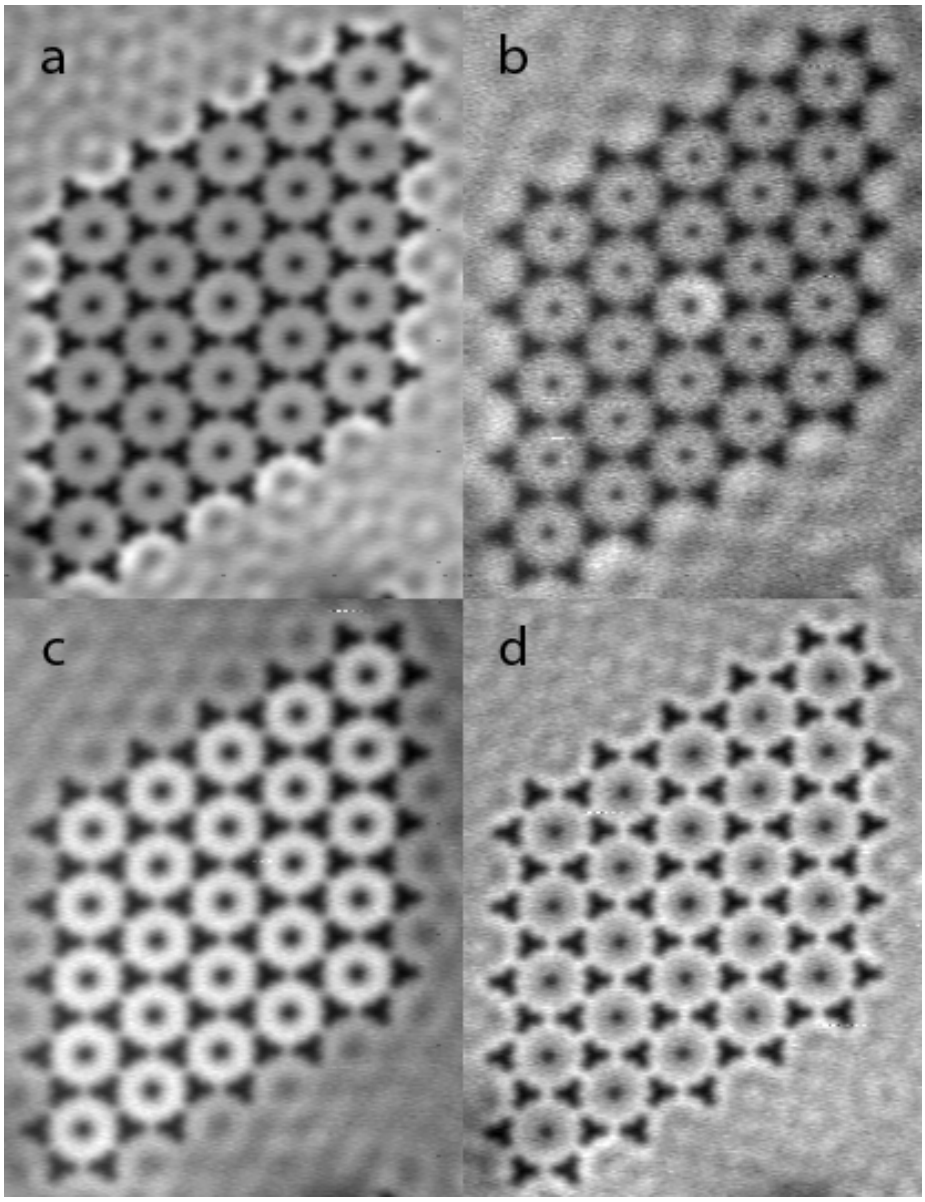

Figure 23: Differential conductance mapping of the trivial Kekulé lattice at 0 V bias(a), -0.225 V bias(b), -0.1 V bias(c), and 0.1 V bias(d).

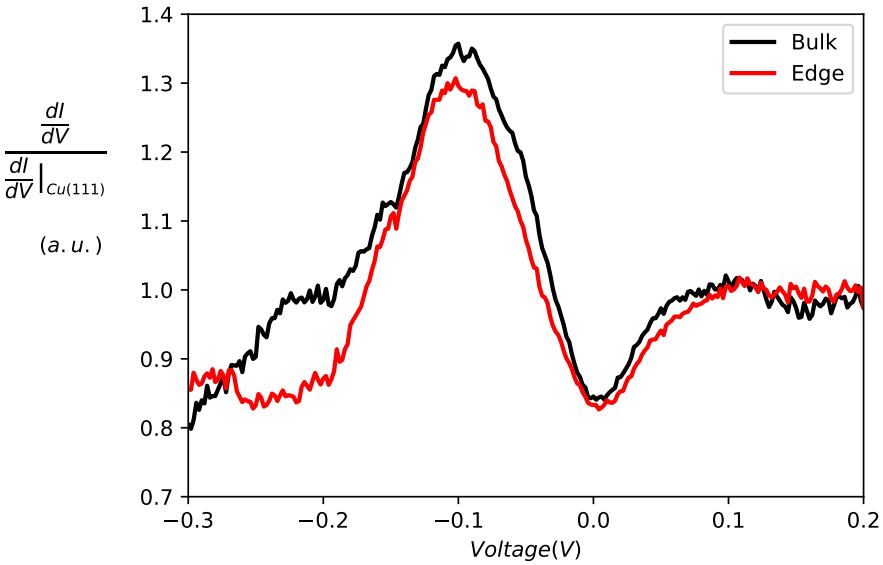

Figure 24: Averaged and normalised differential conductance spectra on the trivial Kekulé lattice. The LDOS is displayed over a bias range of -0.3 to 0.1 V in arbitrary units. The spectrum taken in the bulk is marked **black**, the spectrum on the edge is marked **red**.

Following the simulated result, several modifications were made to the non-trivial Kekulé lattice to show the robustness of the edge [Fig 25]. Three defects were introduced to the lattice as described in **4.1.1** and marked on the differential conductance maps in [Fig 25]: Hopping blocking (cyan), site blocking (red), and boundary removal (yellow). These defects each alter the lattice in a different way but none show an effect great enough to destroy the edge state of the lattice. The dI/dV spectra of the defective lattice also show no reduction in the present edge state, still showing a higher LDOS for the edge than for the bulk in the bias range -0.1 V to 0 V, as was found in the non-defective lattice [Fig 26].
Combining the found edge-states of the Kekulé lattice with $T_0 < T_1$ with pristine, and altered edges, with the lack of an edge state for the Kekulé lattice with hopping ratio $T_0 > T_1$, we find a strong case for the possibility of the creation of artificial edge states using STM. We remain doubtful of the topological qualities of the armchair-edged Kekulé with regard to the theory and simulations.

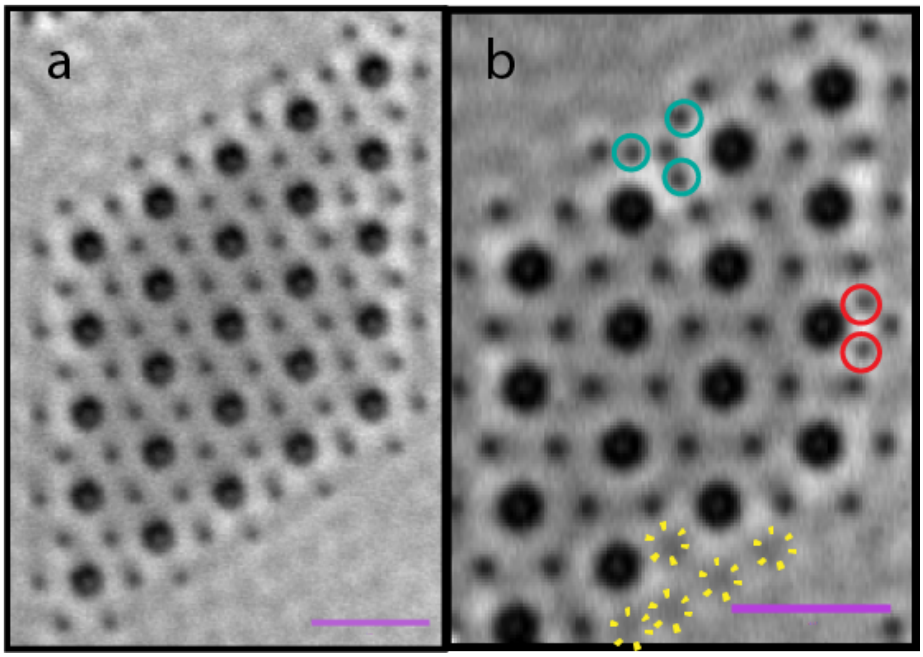

Figure 25: Differential conductance maps of the non-trivial Kekulé lattice unaltered (a) and with the introduction of defects (b) taken at -0.065 V bias. Three types of defects were introduced marked in cyan (hopping blocking), red (site blocking), and yellow (edge removal)

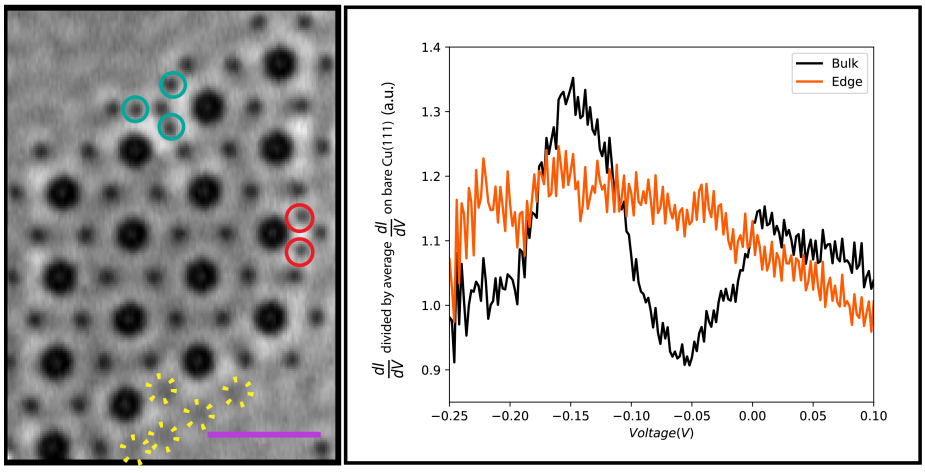

Figure 26: Differential conductance map of the non-trivial Kekulé lattice with defects (left) at -0.065 V bias and the corresponding differential conductance spectrum taken in the bulk (**black**) and at the edge (**orange)**

4.2.2 The Molecule-Zigzag Edge and the Partially-Bearded Edge

The confirmation of the ability to engineer edge states in the artificial lattice of CO on a Cu(111) surface gives great hope to show that the model by Kariyado applies as well. Using the same techniques as for the armchair-edged Kekulé lattice, two additional Kekulé lattices were built; one with a partially-bearded edge, and one with a molecule-zigzag edge.
The partially-bearded lattice was constructed to match the design shown in [Fig 19] using 305 individual CO molecules. The lattice follows the hopping relation $T_0 < T_1$ as it was in the armchair edged, non-trivial Kekulé lattice. In **4.1.2** the minimum in the bulk-gap was shown to be around -0.02 eV, where simulated spectra taken at the edge over the bias range also show a gapped state instead of an edge state. Differential conductance mapping at -0.02 V[Fig 27] also show no visible edge state, displaying relatively uniform intensity throughout the lattice.

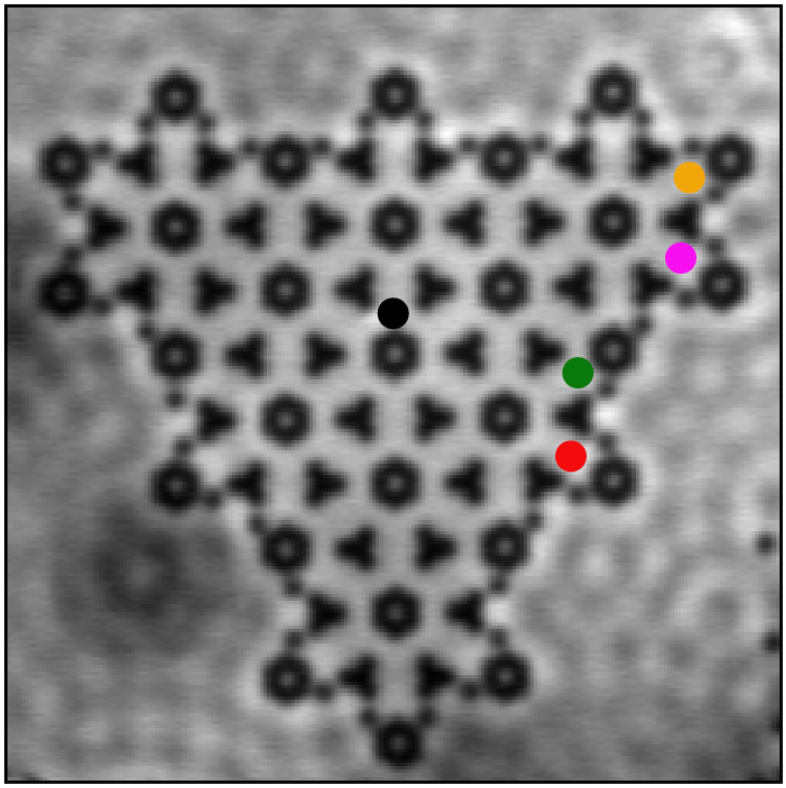

Figure 27: Differential conductance map of the partially-bearded-edged Kekulé lattice taken at -0.02 V. Indicated are different site types; bulk **black**, centre-protrusion **red**, non-protruding-edge **green**, off-centre-protrusion **magenta**, and corner **orange**.

Differential conductance spectra taken on the partially-bearded edge show the same functional LDOS as the simulated result [Fig 28]. The spectra shown are non-normalised to maintain clarity. The model by *Kariyado* appears to be a functional way of determining the topology of a system so far. To expand on this the partially-bearded lattice was converted to the molecule-zigzag lattice by adding to the edges of the partially-bearded lattice for a total 522 individual CO molecules.

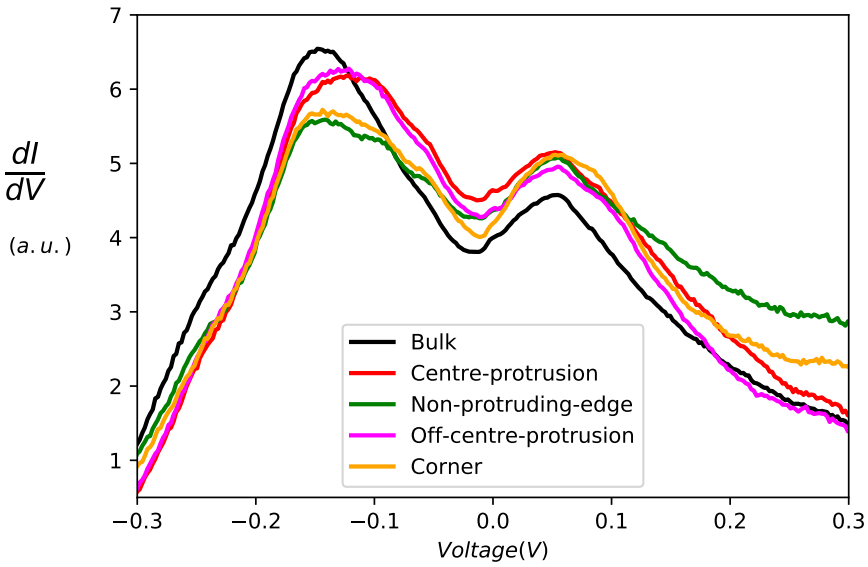

Figure 28: Non-normalised differential conductance spectra taken on the partially-bearded Kekulé lattice shown in the -0.3 V to 0.3 V bias range. Colours correspond to colours indicated in [Fig 27].

The molecule-zigzag edged lattice has the same relation of hopping parameters as the partially-bearded lattice, $T_0 < T_1$, thus the topology of the system should be solely dependant on the symmetry presented by the shape of the edge introducing the desired opposing mirror-winding numbers for topological behaviour [18]. Simulated results show the presence of a clear edge state per [Fig 16], with a greatest difference of LDOS around -0.01 eV [Fig 18d]. Differential conductance mapping show the clear presence of heightened DOS at this energy [Fig 29], and a comparative image shows a clear presence of the edge state in the molecule-zigzag edge while it is clearly absent in the partially-bearded lattice. The intensity of the edge varies throughout the differential conductance map, showing lower intensity in the lower left corner of [Fig 29] than in the other corners. We attribute this to a nearby subsurface defect, altering the base copper surface state. Thus it appears the mirror-winding number influences the presence of the topological edge state as much as proposed by Kariyado. Dif-

ferential conductance spectra on the molecule-zigzag show the same behaviour as predicted, with a clearly present edge state in the bulk gap of the lattice [Fig 30]. The simulated bulk-gap from -0.1 V to 0 V bias is presented in the molecule-zigzag lattice, as well as the crossing of the edge LDOS above the gap. The spectra were normalised on the copper background to show a distinct increase in LDOS over the 2DEG and averaged over multiple spectra to achieve an average LDOS.

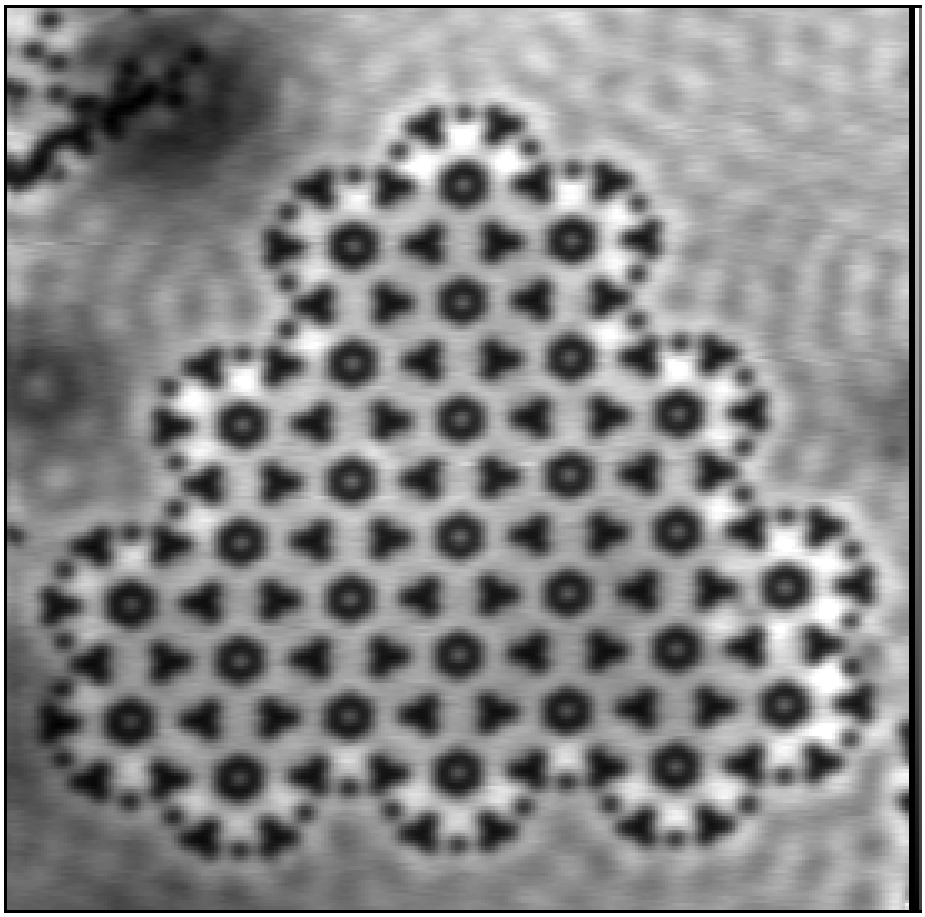

Figure 29: Differential conductance mapping of the molecule-zigzag-edged Kekulé lattice at -0.01 V bias.

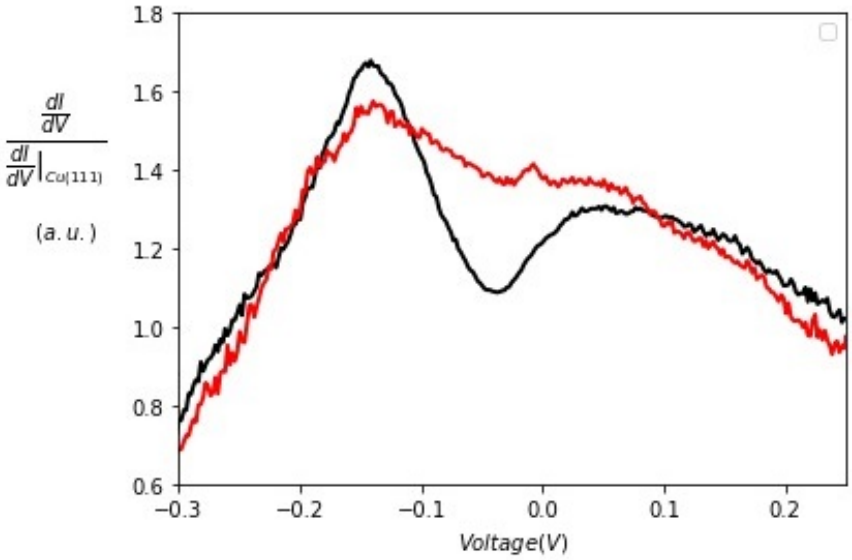

Figure 30: Averaged differential conductance spectra of the molecule-zigzag-edged Kekulé lattice. Spectra of the bulk are shown in **black**. Spectra of the edge are shown in **red**

On first look, the different types of sites noted in **4.2.2** do not appear to vary as strongly in intensity as the simulated LDOS plot would imply. While the variance between a neighbour-type-site and a zigzag-site is predicted to be great but not overwhelming, the variance in DOS between the corner sites and the other types was shown to be great, with a steep dip owning to the trimer character of the edge site. Differential conductance spectra should show a difference in LDOS on the specific types of site, even if they are not visible in the differential conductance maps. We observe that, while the edge state is clearly present, not all edge sites are equivalent [Fig.31] [Fig. 32]. Within the molecule-zigzag-edged lattice the NN-hopping is not equivalent on all sites as shown in theory by Kariyado [18] and simulations [Fig. 16]. We see this effect in differential conductance spectra by a light variation in LDOS for the different sites indicated. While in theory the central-corner type site should have the lowest LDOS, it is only negligibly different from the LDOS of the neighbour site [18]. The LDOS of the non-portruding-edge site lies higher than that of the neighbour- and corner type sites, which is in accordance with theory [Fig 10][18]. We consider the deviation from theory on the neighbour and corner sites to be an effect of the triangular lattice used. Where theoretical calculations by Kariyado are done on ribbons of artificial lattices, the confined structure of the artificial Kekulé effects next-nearest-neighbour hopping, which is neglected in theory for its overall equality throughout the theoretically infinite ribbon [18].

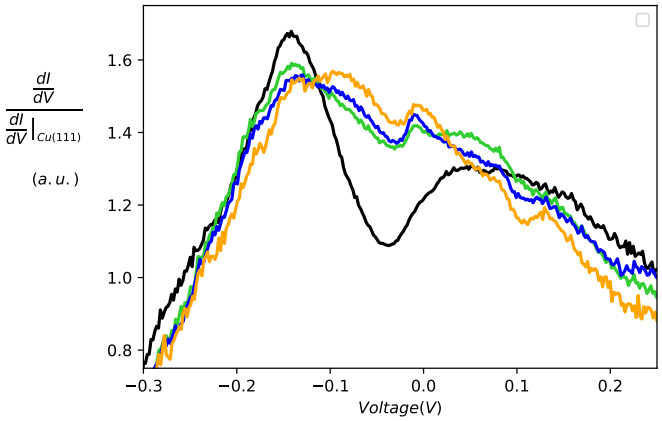

Figure 31: Averaged differential conductance spectra of the molecule-zigzag on sites indicated in [Fig. 32]. Every site was averaged over multiple spectra and normalised against the copper background.

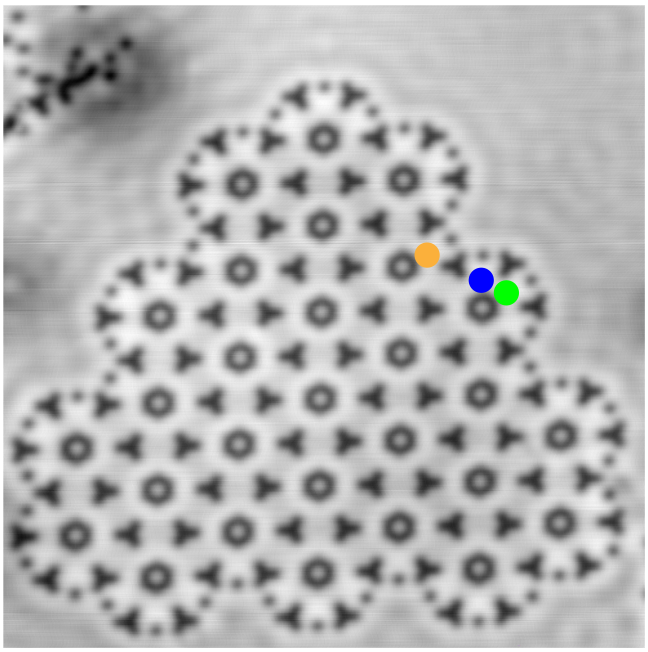

Figure 32: Topograph of the molecule-zigzag edged Kekulé lattice with different site-types indicated in **green** (central corner), **blue** (neighbour) and **orange** (non-portruding edge)

Further, we note that the simulations in [Fig 18c] do show a greater match to the differential conductance spectra taken than [Fig 18d]. On a lattice of this form without blocking the LDOS of the corner, neighbour, and zigzag sites matches far more than when blockers are introduced, which would case a more defined splitting of the individual sites. We must consider the possibility that even with blockers the sites at the edges experience the effects of interactions with the 2DEG, forming a more uniform edge state. Aside from the qualities in the lattice itself, the effect of a tip that was less than optimal for spectroscopy should not be neglected. The influence of the tip shape was shown in **2.2**, and variations there in can have far reaching consequences for the spectral shape obtained.

The topology of the lattice was checked for robustness via the introduction of defects at the edge, with three different defects introduced; a single site blocking in a corner site, blocking of two neighbour sites, and blocking of a single neighbour site [Fig 33 a-d]. On all dI/dV maps the edge state appears to persist, differing in intensity throughout the lattice. The single defect on the corner site does not alter the the presence of an edge with regard to the pristine lattice, showing the same heightened intensity along the edge indicative of an edge state. The intensity shown appears lesser in the lower left corner of the lattice, congruent with the lowered intensity due to a present subsurface defect seen in the pristine lattice [Fig 29]. The single defect here was placed first on a corner-type site as a site-blocking defect[Fig 33b]. The edge state was observed to be intact after the introduction of this defect. Blocking of two neighbour-sites while the corner-site remained intact also allowed the edge state to remain intact [Fig 33c], again showing only lower intensity of the edge around the lower-left corner adjacent to the subsurface defect. The final defect introduced was again a single scatterer, placed to remove any form of local symmetry in the lattice [Fig 33d]. The placement of a single CO removes all symmetry-axis, breaking local symmetry completely. This defect also shows no influence on the edge state, which is still comparable to its form in both the pristine lattice and with other defects introduced.

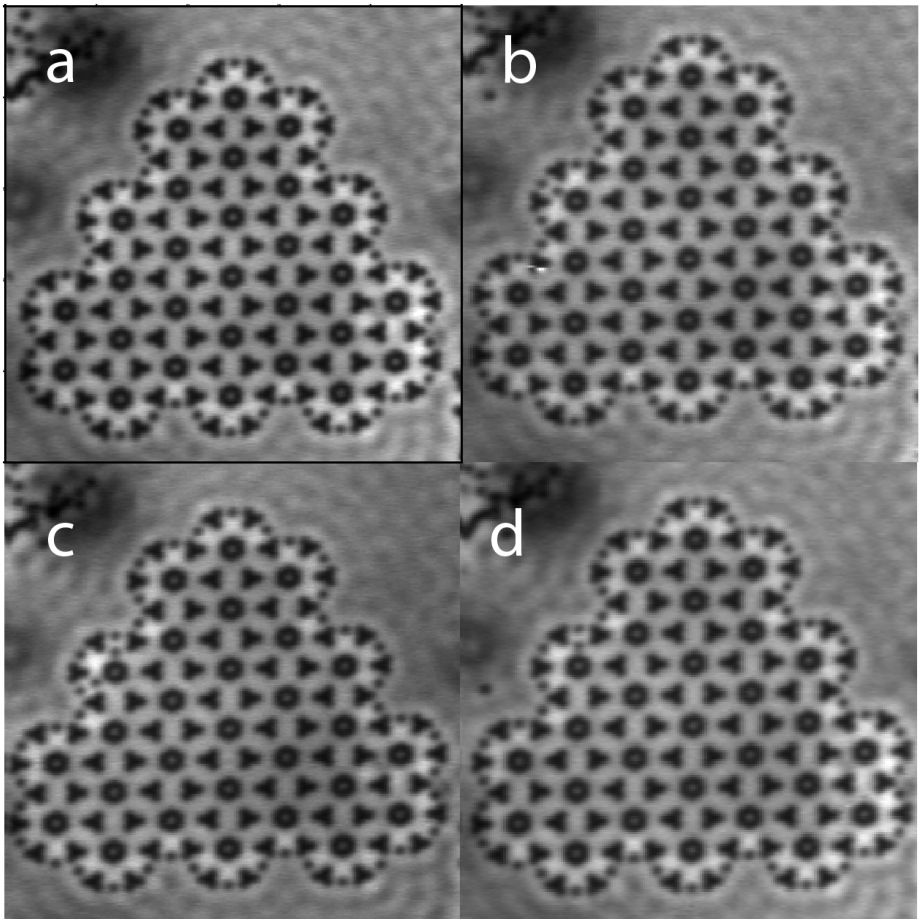

Figure 33: differential conductance maps of the molecule-zigzag-edged Kekulé lattice at -0.04 V bias with no defect (a), one corner-site blocking scatterer (b), two neighbour-site blocking scatterers (c), and a single neighbour blocking defect (d).

The molecule-zigzag-edged Kekulé thus appears to be a robust topological insulator from differential conductance mapping. To verify this differential conductance spectra on all defects were taken, as well as differential conductance spectra on opposite sites of each defected lattice to show the persistence of the edge state across the lattice. Here we see that heightened LDOS of the edge remains for the gapped state of the bulk, both around the defects and on the opposite sites of the lattice. For all defects the edge state is visible in the dI/dV spectroscopy as in dI/dV mapping. We find the presence of edge states in the artificial lattices depending on the hopping parameters and edge termination satisfactorily supported by experiments.

While it would have been prudent to test for topological edge states in the lattices with the partially-bearded and molecule-zigzag edge with inverted hopping parameter ratios as described by Kariyado, time constraints withheld us from doing so. While this is a crucial part of the research into the topological insulator, we do not believe that findings on these lattices will disprove the findings above, but only strengthen these. The findings above were done with a great eye for consistency, but the methodology behind an STM does not always allow for pure consistency. A wide array of variables in the STM may influence the results achieved by virtue of being, while the researcher has no control over these variables. We consider the main variables such as pressure and temperature to be of negligible influence on the results achieved, while variations in tip-shape and specific variations in the surface have been normalised for as much as possible to reduce their specific influence. The great agreement of the experimental results with theory and simulations was expected for a system that is invariably lifted from the realm of theory into reality. We attempted to remain as true to the theory as possible. Designs for lattices that were based on theory never strayed from theory. The designs were kept consciously and consistently close to the theory to be able to employ the theory as best we could.

5 Conclusion

The artificial armchair-Kekulé lattices were built using CO molecules as electron scatterers on the 2DEG present on a Cu(111) surface. The lattices were built in configurations with hopping parameter ratio T_0/T_1 tuned to be greater and lower than 1 to attempt to achieve the creation of topological edge states. Differential conductance mapping and spectroscopy on both Kekulé lattices confirmed the presence of edge states for the hopping parameter ratio $T_0/T_1 < 1$, and the absence of edge states for hopping parameter ratio $T_0/T_1 > 1$. These results are in line with theoretical findings and are considered a confirmation of proposed engineering methods for edge states. In accordance with simulations of the bandstructure of the armchair-edged lattice with edge states present, we do not consider this lattice to have topological edge states. This is in accordance with theory on the influence of the mirror winding number on the topological edge state. Using the same methods, artificial Kekulé lattices with hopping parameter ratios $T_0/T_1 < 1$ with both partially-bearded and molecule-zigzag edges were built on the 2DEG of the Cu(111) surface to assess the influence of the mirror-winding number on the presence of topological edge states. Using differential conductance mapping and spectroscopy the partially-bearded lattice was determined to contain no topological edge states, in accordance with theory. The molecule-zigzag edged lattice was shown to contain topological edge states at a -40 mV bias. These edge states were robust when introducing defects to the lattice and show that in addition to the hopping parameter ratio T_0/T_1 the mirror-winding number is crucial in the engineering of topological edge states. We find the building of artificial lattices with topological edge states viable in practice and in strong agreement with theory.

6 Outlook

While we consider it convincingly shown that it is possible to engineer topological edge states in lattices by adjusting the internal hopping parameters of artificial lattices, as well as tuning the edge to adjust the mirror winding number, the journey into the unexplored fields of topological insulators is far from over. Time fell short to apply final tests on the mirror winding numbers, and it is suggested to complete the experiments on the partially-bearded and molecule-zigzag edges. Here we should invert the hopping parameters to create lattices with the hopping ratio $T_0/T_1 > 1$, which should not have a topological edge state for the armchair edge but promises one for the partially-bearded edge, while removing it for the molecule-zigzag edge [18]. This would confirm the strong influence of the mirror-winding number on the topological insulator. The topological insulator, and artificial lattices as a whole are still in their infancy, but shows promise to rapidly become one of the hottest topics in modern day science. With the ability to create nano-scale highly conductive systems, highly theoretical concepts such as quantum computing are brought closer to reality than they have ever been before. While the topic remains fundamental at its core for the foreseeable future, we hope to have joined the first steps made in theory with practical results to function as a basis for further study into this infinitely fascinating field.

7 Acknowledgements

First and foremost, I would like to thank Saoirsé Freeney, for her supervision of this master's project. Her scientific expertise, as well as her humour and ability to dream big and motivate others to do so, made for an excellent year down in the basement. Many thanks go to my supervisor Ingmar Swart, who dreams big as well and helms the STM group at Utrecht University, personally paving a path into the future. This research would not have been possible without the help of the department of Theoretical Physics, whose simultions and calculations guided us in times of need. Many thanks go to Jette van den Broeke for her tireless work on these calculations, and her supervisor Cristiane Morais Smith. Team Kelder is luckily more than just three members, and is as a unit greater than the sum of its parts. Thanks go to Lisanne Knijff and Sam Borman, who were supervised by Saoirsé for their bachelor's degree and brought much joy and many laughs to the basement. My office-mate and fellow master's student Jesper Moes, who has already taken up his PhD position at the Swart-group, is thanked for his endless banter and strong insights in between, as is his supervisor Thomas Gardenier. No acknowledgement in the basement is complete without mentioning Marlou Slot, as without her expertise and endless energy the basement would have fallen long ago. Further insights and classical Dutch 'gezelligheid' were provided by the next generation of master's students; Jan Cuperus, Rian Ligthart, Tomas Meerwijk, and Jos Mulkens. Fellow PhD's Christiaan Post and Peter Jacobse provided humorous background noise playing table football. Luckily my support system was not limited to Utrecht University, and I could count on friends on all sides during my thesis. Thank you, my housemates Cyrano, Saritha, and Tim, for the homely house you provide, thank you Ties and Mickey for the deep phylosophical insights we share, and thanks to all 18 other members of HC Houten H4, for sticking with my eternal frustration in these trying times. Thank you Bram, for finding me and letting me find you. Last, but by no possible standard least, I would like to thank my family dearly for all the support in every way I needed it. Trudy, Jan Egbert, and Sterre, you are a wonderful family to be a part of, and the fresh air provided by walks with Kaira and Chachí was always welcome.

Down in the Basement
A year spent in elation
A bittersweet end

8 References

[1] Gerd Binnig, Heinrich Rohrer, Ch Gerber, and Edmund Weibel. Surface studies by scanning tunneling microscopy. *Physical review letters*, 49(1):57, 1982.

[2] Gerd Binnig and Heinrich Rohrer. Scanning tunneling microscopy—from birth to adolescence. *reviews of modern physics*, 59(3):615, 1987.

[3] L Bartels, G Meyer, and K-H Rieder. Basic steps of lateral manipulation of single atoms and diatomic clusters with a scanning tunneling microscope tip. *Physical Review Letters*, 79(4):697, 1997.

[4] AJ Heinrich, CP Lutz, JA Gupta, and DM Eigler. Molecule cascades. *Science*, 298(5597):1381–1387, 2002.

[5] Kenjiro K Gomes, Warren Mar, Wonhee Ko, Francisco Guinea, and Hari C Manoharan. Designer dirac fermions and topological phases in molecular graphene. *Nature*, 483(7389):306, 2012.

[6] SN Kempkes, MR Slot, SE Freeney, SJM Zevenhuizen, D Vanmaekelbergh, I Swart, and C Morais Smith. Design and characterization of electronic fractals. *arXiv preprint arXiv:1803.04698*, 2018.

[7] A. H. Castro Neto, F. Guinea, N. M. R. Peres, K. S. Novoselov, and A. K. Geim. The electronic properties of graphene. *Rev. Mod. Phys.*, 81:109–162, Jan 2009.

[8] Dmytro Pesin and Allan H MacDonald. Spintronics and pseudospintronics in graphene and topological insulators. *Nature materials*, 11(5):409, 2012.

[9] Qi-Kun Xue. Nanoelectronics: A topological twist for transistors. *Nature nanotechnology*, 6(4):197, 2011.

[10] Sergey Bravyi and Alexei Kitaev. Universal quantum computation with ideal clifford gates and noisy ancillas. *Physical Review A*, 71(2):022316, 2005.

[11] Joel E Moore. The birth of topological insulators. *Nature*, 464(7286):194, 2010.

[12] Yuqi Xia, Dong Qian, David Hsieh, L Wray, Arijeet Pal, Hsin Lin, Arun Bansil, DHYS Grauer, Yew San Hor, Robert Joseph Cava, et al. Observation of a large-gap topological-insulator class with a single dirac cone on the surface. *Nature physics*, 5(6):398, 2009.

[13] G. Binnig and H. Rohrer. Scanning tunneling microscopy. *Surface Science*, 126(1):236 – 244, 1983.

[14] G. Binnig and H. Rohrer. Surface imaging by scanning tunneling microscopy. *Ultramicroscopy*, 11(2):157 – 160, 1983.

[15] Marlou R Slot, Thomas S Gardenier, Peter H Jacobse, Guido CP van Miert, Sander N Kempkes, Stephan JM Zevenhuizen, Cristiane Morais Smith, Daniel Vanmaekelbergh, and Ingmar Swart. Experimental realization and characterization of an electronic lieb lattice. *Nature physics*, 13(7):672, 2017.

[16] Chang-Yu Hou, Claudio Chamon, and Christopher Mudry. Electron fractionalization in two-dimensional graphenelike structures. *Phys. Rev. Lett.*, 98:186809, May 2007.

[17] Shi-Liang Zhu, Baigeng Wang, and L-M Duan. Simulation and detection of dirac fermions with cold atoms in an optical lattice. *Physical review letters*, 98(26):260402, 2007.

[18] Toshikaze Kariyado and Xiao Hu. Topological states characterized by mirror winding numbers in graphene with bond modulation. *Scientific reports*, 7(1):16515, 2017.

[19] Md Nurul Huda. *Epitaxial growth of lateral graphene / hexagonal boron nitride heterostructures*. PhD thesis, 10 2016.

[20] G. Hörmandinger. Imaging of the cu(111) surface state in scanning tunneling microscopy. *Phys. Rev. B*, 49:13897–13905, May 1994.

[21] J. Tersoff and D. R. Hamann. Theory of the scanning tunneling microscope. *Phys. Rev. B*, 31:805–813, Jan 1985.

[22] Robert J Celotta, Stephen B Balakirsky, Aaron P Fein, Frank M Hess, Gregory M Rutter, and Joseph A Stroscio. Invited article: Autonomous assembly of atomically perfect nanostructures using a scanning tunneling microscope. *Review of Scientific Instruments*, 85(12):121301, 2014.

[23] Joseph A Stroscio and DM Eigler. Atomic and molecular manipulation with the scanning tunneling microscope. *Science*, 254(5036):1319–1326, 1991.

[24] L. Bartels, G. Meyer, and K.-H. Rieder. Basic steps involved in the lateral manipulation of single co molecules and rows of co molecules. *Chemical Physics Letters*, 273(5):371 – 375, 1997.

[25] Gerhard Meyer, Ludwig Bartels, and Karl-Heinz Rieder. Atom manipulation with the stm: nanostructuring, tip functionalization, and femtochemistry. *Computational materials science*, 20(3-4):443–450, 2001.

[26] Long-Hua Wu and Xiao Hu. Topological properties of electrons in honeycomb lattice with detuned hopping energy. *Scientific reports*, 6:24347, 2016.

[27] Shinsei Ryu, Andreas P Schnyder, Akira Furusaki, and Andreas WW Ludwig. Topological insulators and superconductors: tenfold way and dimensional hierarchy. *New Journal of Physics*, 12(6):065010, 2010.

[28] J.J. van den Broeke. Inhouse calculations, 2018. Utrecht University department of Theoretical Physics.

9 Supplementary information

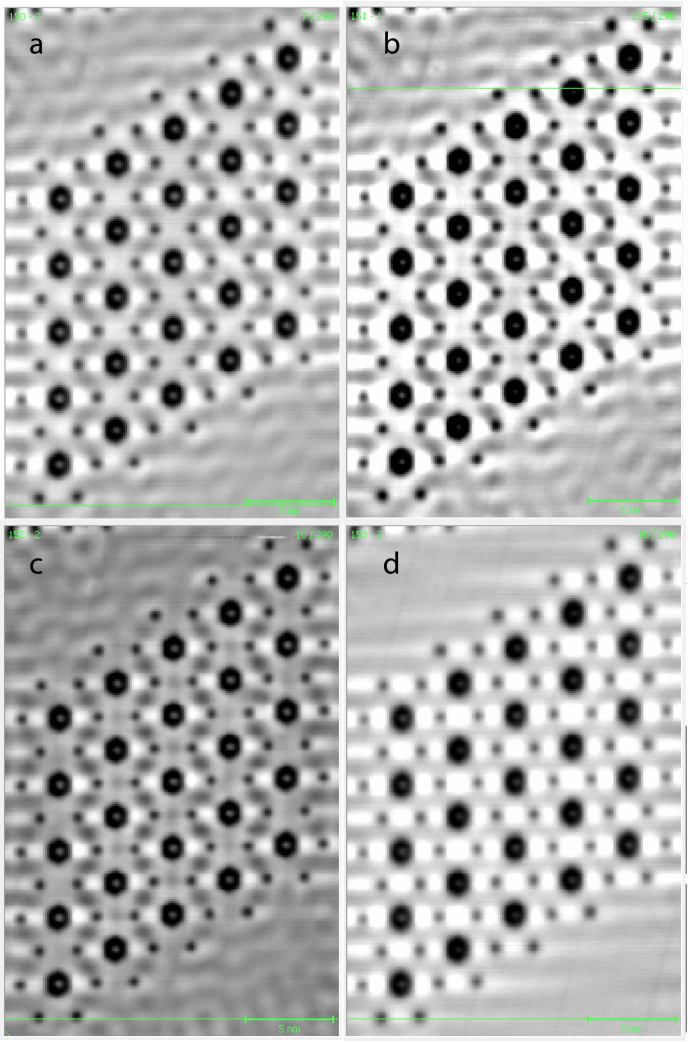

Supplementary 1: Topographic images of the armchair-edged Kekulé lattice with hopping ratio $T_0/T_1 < 1$ at -0.1 V (a), -0.075 V (b), -0.01 V (c), and -0.4 V (c). While the edge state is not clearly shown as in differential conductance mapping, clear distinctions in intensity at varying energies can be seen.

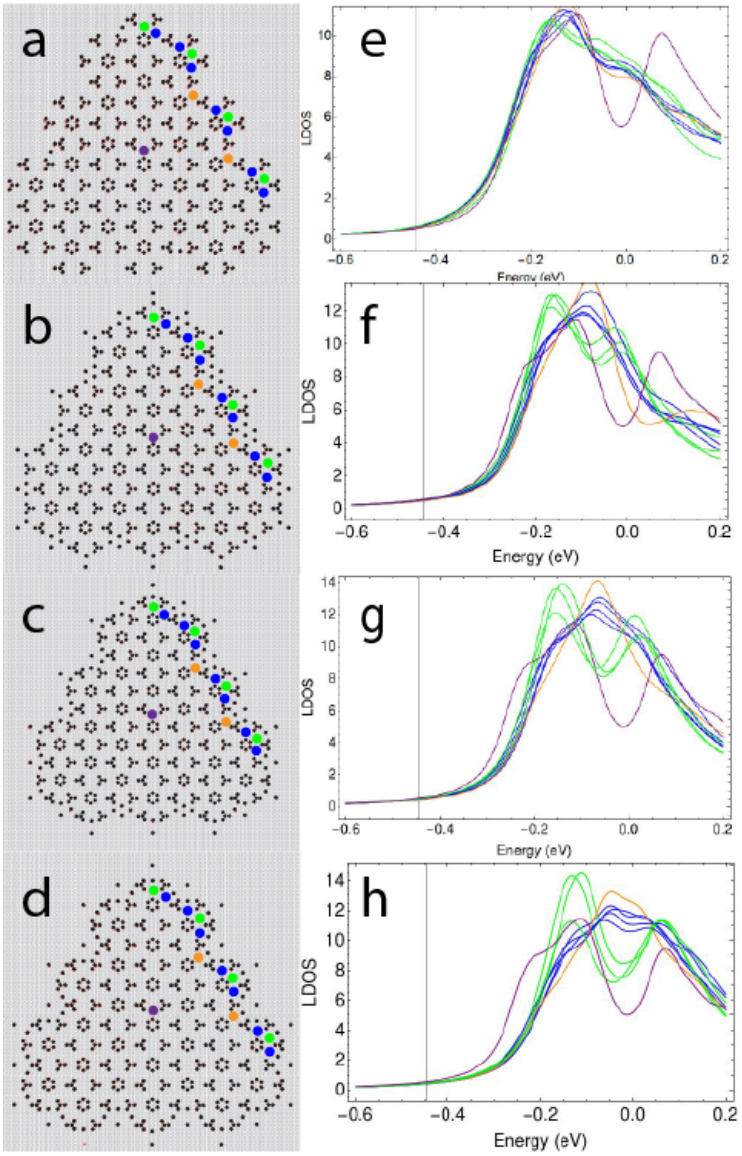

Supplementary 2: Progression of the spectral shape with the introduction of blockers to the molecule-zigzag edged Kekulé lattice. With a closer proximity of CO blockers to the artificial sites the spectral shape is reshaped to match the TB-calculated LDOS in the lattice.

Supplementary 3: Energy solutions for dimers and trimers

To find the eigenvalue for the energy of the dimer molecule, one only needs to solve a simple determinant;

$$det\begin{vmatrix}\alpha - E & \beta \\ \beta & \alpha - E\end{vmatrix} = 0 \tag{10}$$

Where the solution $E_{\pm} = \alpha \pm \beta$ is easily obtained. The dimer shows two distinct energy levels that are separated far from each other, with no trivial solution E_0. In a trimer molecule we apply the determinant;

$$det\begin{vmatrix}\alpha - E & \beta & 0 \\ \beta & \alpha - E & 0 \\ 0 & \beta & \alpha - E\end{vmatrix} = 0 \tag{11}$$

Where to remain consistent with TB for our simulations we set the next-nearest-neighbour hopping to 0. Here we obtain energy solutions for $E \neq 0$ and a solution for $E = 0$ as $E_{\pm} = \alpha \pm \sqrt{2}\beta$ and $E_0 = \alpha$. The existence of an E_0 state requires the band crossing for conductance and thus shows a topological edge state for the system applied.